

RESULTS AND DISCUSSION

1. The spectroscopic properties of crude dyes extracted from plants and *Monascus* rice cultures and a ruthenium complex (N3) dye

1.1 UV-Vis absorption spectra

1.1.1 The absorption spectra of crude dyes extracted from roselle, turmeric and *Monascus* red and *Monascus* yellow rice cultures in ethanol solution are shown in Figure 20.

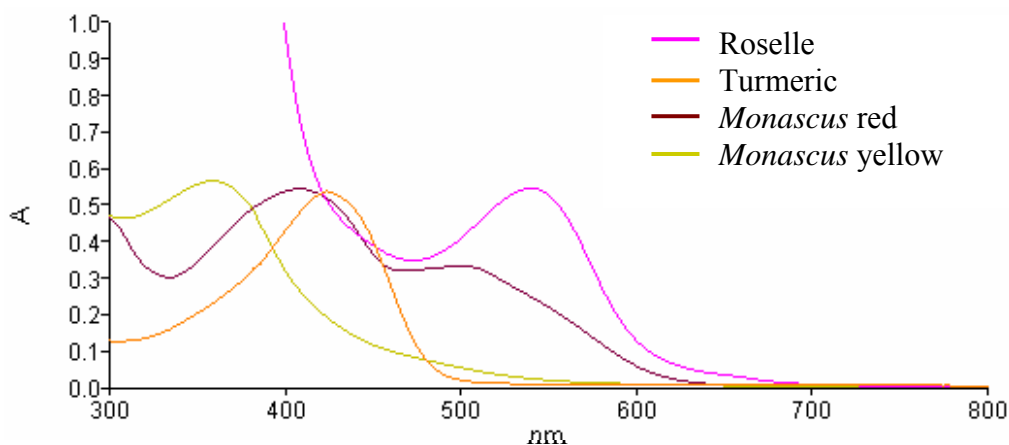


Figure 20 The absorption spectra of crude dyes extracted from plants and *Monascus* rice cultures in ethanol solution.

From Figure 20, it can be seen that the absorptions of roselle and turmeric in ethanol solutions are in the range 300-700 nm (λ_{\max} 540 nm) and 300-510 nm (λ_{\max} 424 nm) which depict the core constituent of anthocyanin and curcumin, respectively. The absorptions of *Monascus* red and *Monascus* yellow are in the range 300-620 nm (λ_{\max} 410 and 500 nm) and 300-550 nm (λ_{\max} 360 nm), respectively. These results show that these dyes are useful for sensitizing TiO₂ solar cells and roselle and *Monascus* red extracts absorb wider range of the photospectrum than turmeric and *Monascus* yellow extracts.

1.1.2 The absorption spectra of mixture of dye extracts in ethanol solution are shown in Figure 21- Figure 26.

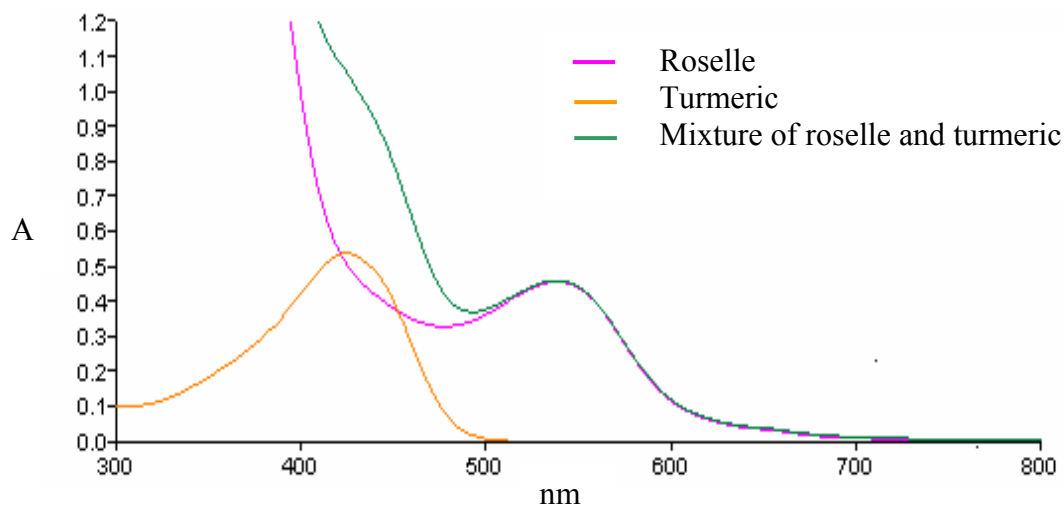


Figure 21 The absorption spectra of roselle, turmeric and mixture of roselle and turmeric extracts in ethanol solution.

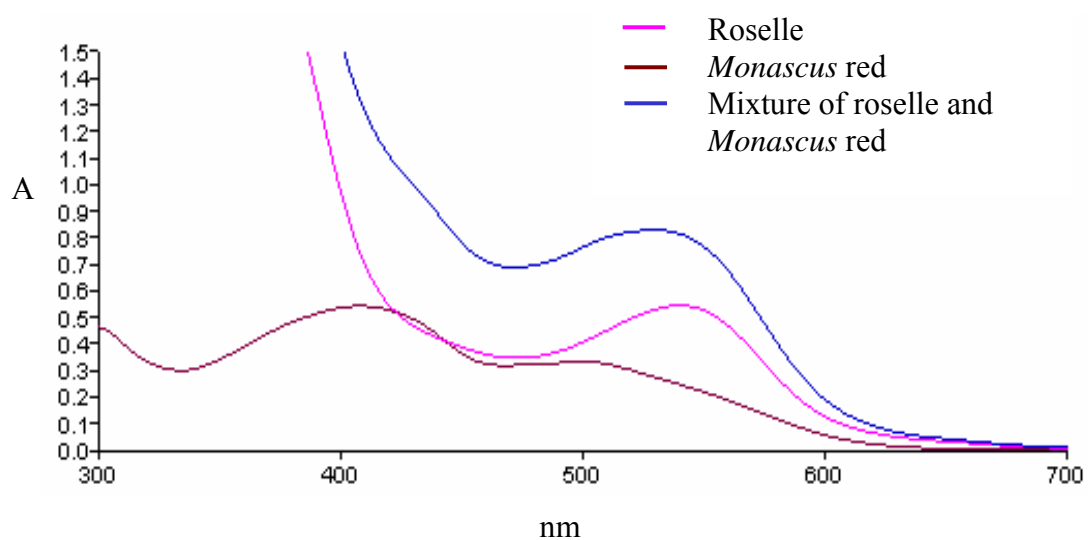


Figure 22 The absorption spectra of roselle, *Monascus* red and mixture of roselle and *Monascus* red extracts in ethanol solution.

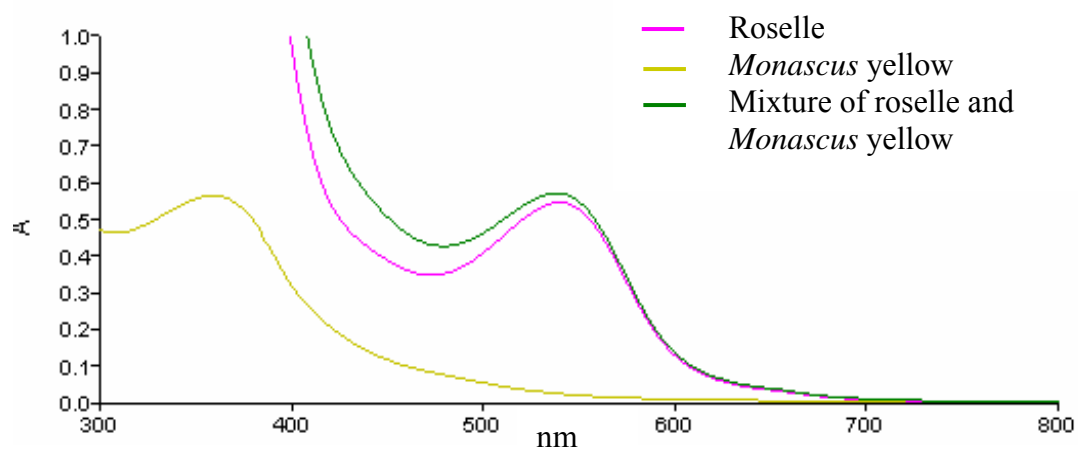


Figure 23 The absorption spectra of roselle, *Monascus* yellow and mixture of roselle and *Monascus* yellow extracts in ethanol solution.

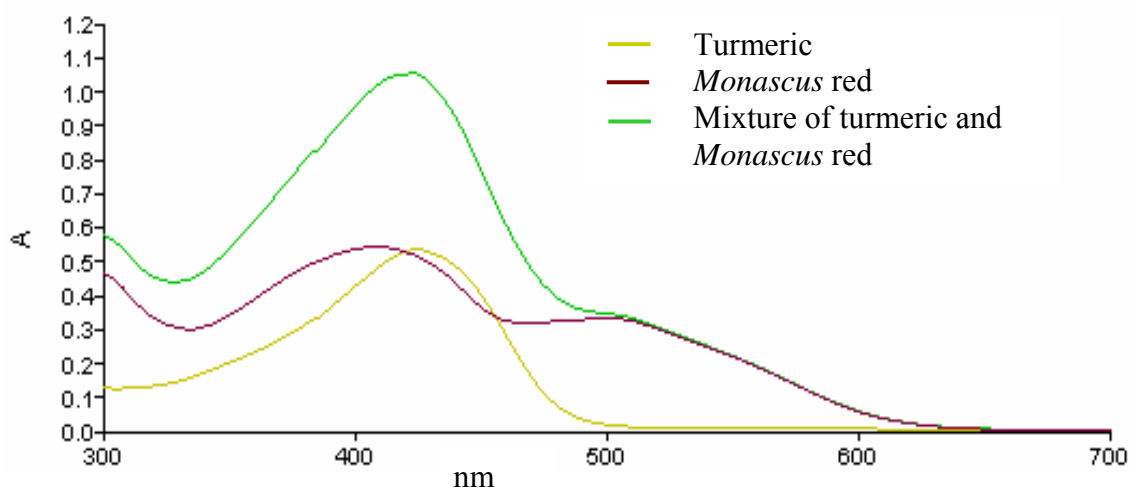


Figure 24 The absorption spectra of turmeric, *Monascus* red and mixture of turmeric and *Monascus* red extracts in ethanol solution.

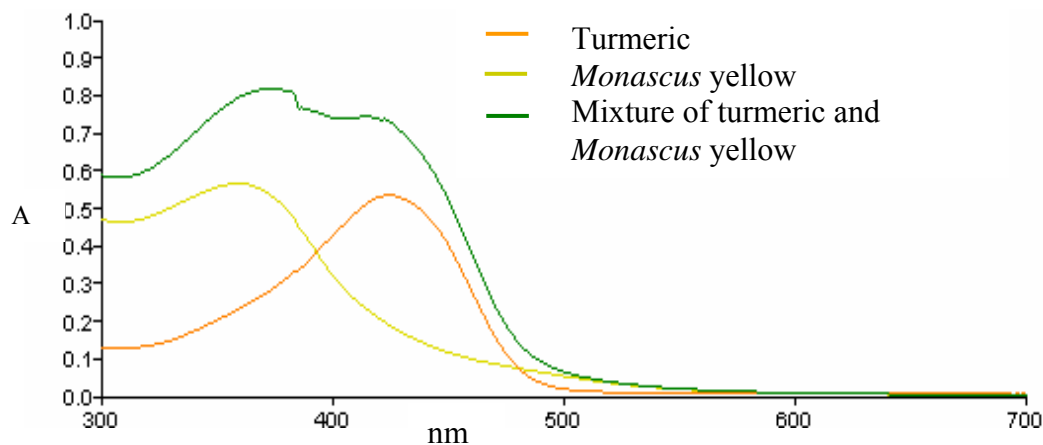


Figure 25 The absorption spectra of turmeric, *Monascus* yellow and mixture of turmeric and *Monascus* yellow extracts in ethanol solution.

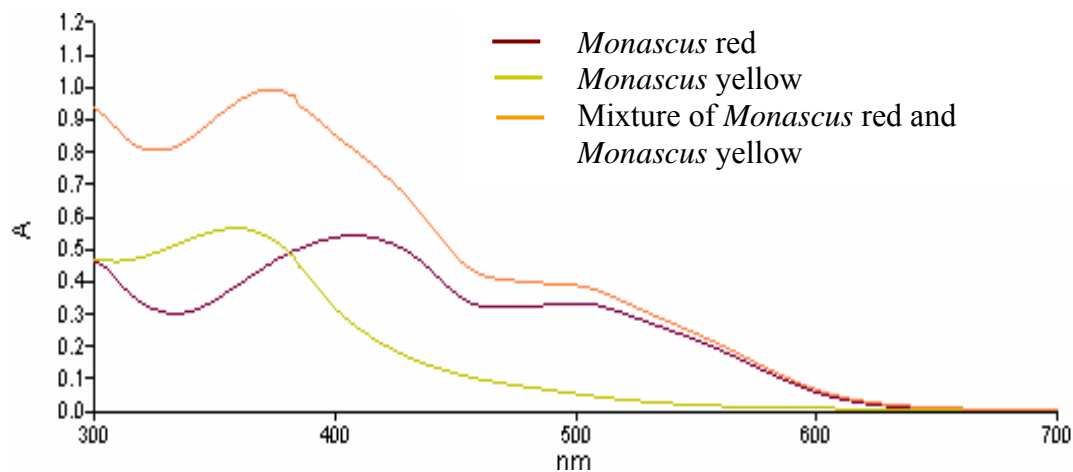


Figure 26 The absorption spectra of *Monascus* red, *Monascus* yellow and mixture of *Monascus* red and *Monascus* yellow extracts in ethanol solution.

From Figure 21- Figure 26, the absorption intensities of combinations of mixture of dye extracts are higher than those of the single dyes, while the absorption range of each combination is up to the range of the single dye of wider range. These results can be used to predict the best combination of mixture dyes that would be the best sensitizer on account of wider range of higher absorption intensity of the mixed dyes.

1.1.3 The absorption spectrum of [Ru(4,4'-dicarboxylic bipyridyl)₂(NCS)₂] or N3 dye in ethanol solution is shown in Figure 27. The absorption range is 300-720 nm with maximum absorption (λ_{\max}) wavelength at 314, 400 and 536 nm. The intense and broad range of absorption depict the effectiveness of sensitization, as a result, the N3 dye is one of the most effective photosensitizer in dye-sensitized solar cell.

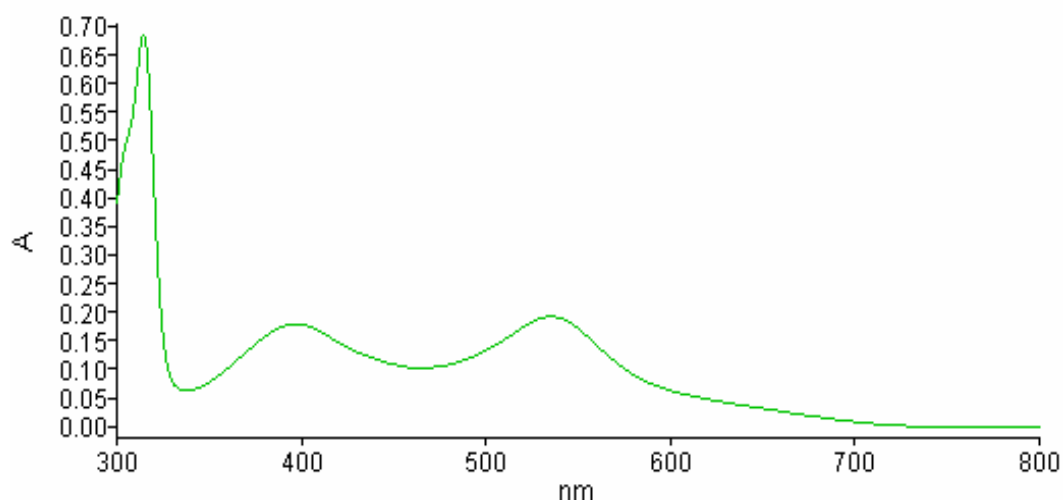


Figure 27 The absorption spectrum of [Ru(4,4'-dicarboxylic bipyridyl)₂(NCS)₂] or N3 dye in ethanol solution.

1.2 Fluorescence spectra

1.2.1 The fluorescence spectra of crude dyes extracted from roselle, turmeric and *Monascus* red and *Monascus* yellow rice culture, in ethanol solution are shown in Figure 28 – Figure 31. The excitation wavelength of crude dyes extracted from roselle, turmeric and *Monascus* red and *Monascus* yellow rice culture are 380, 420, 470 and 410 nm, respectively. All four dyes display a strong fluorescence emission at room temperature.

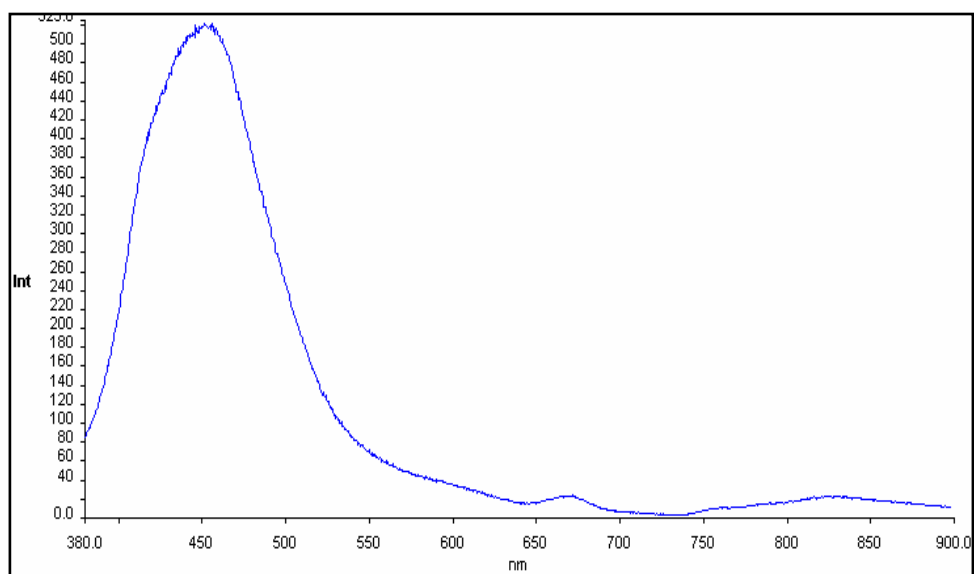


Figure 28 The fluorescence spectrum of crude dye extracted from roselle in ethanol solution. The excitation wavelength was 380 nm.

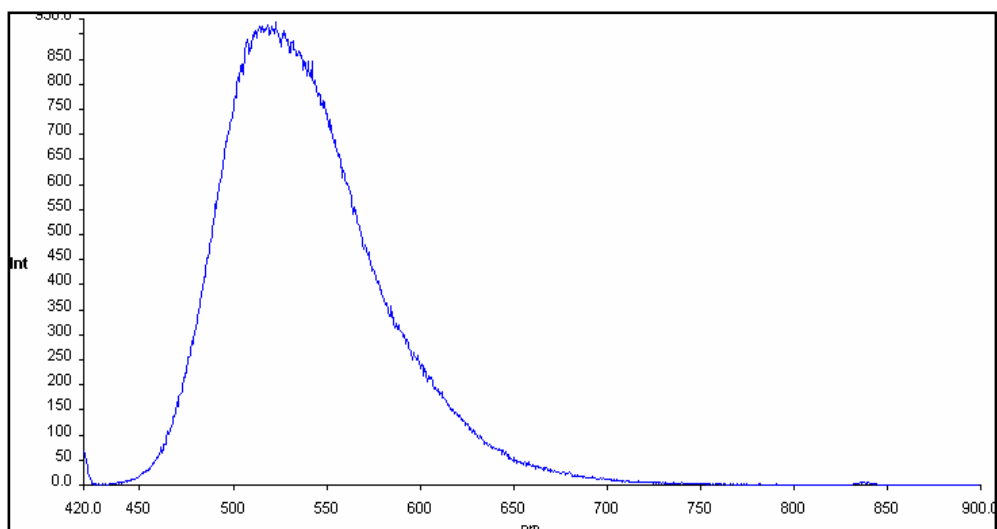


Figure 29 The fluorescence spectrum of crude dye extracted from turmeric in ethanol solution. The excitation wavelength was 420 nm.

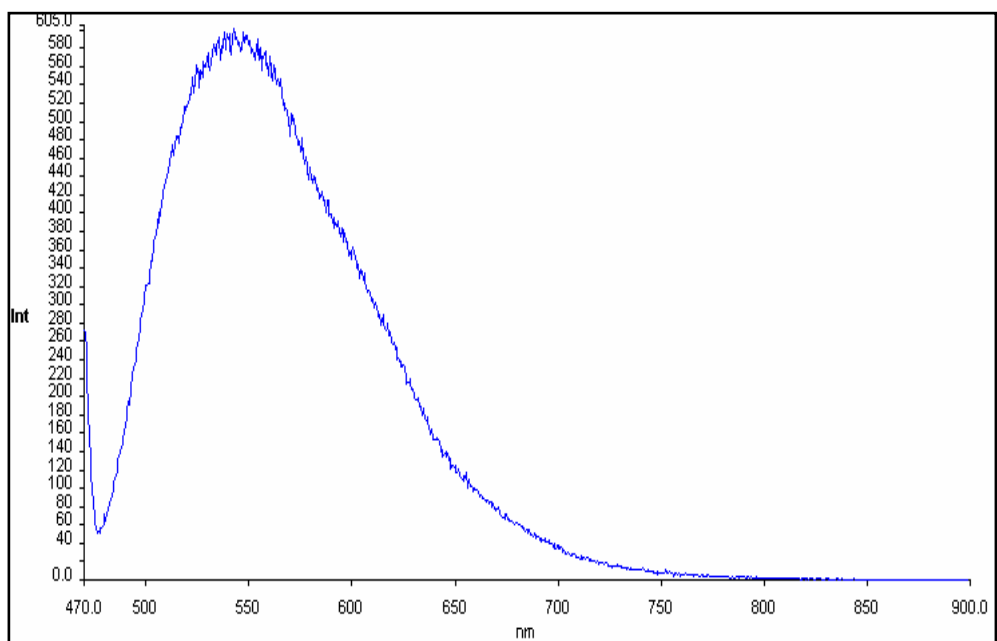


Figure 30 The fluorescence spectrum of crude dye extracted from *Monascus* red rice culture in ethanol solution. The excitation wavelength was 470 nm.

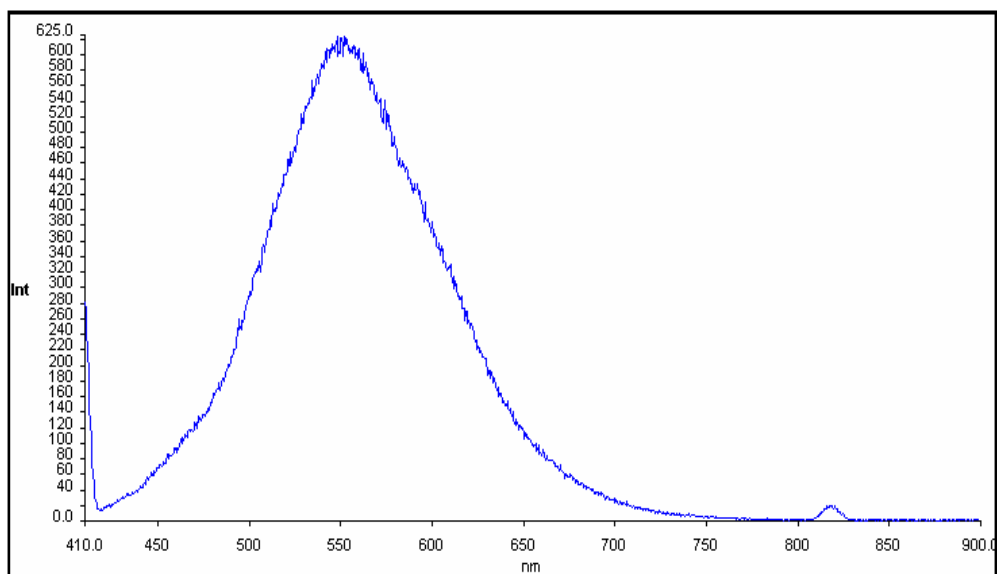


Figure 31 The fluorescence spectrum of crude dye extracted from *Monascus* yellow rice culture in ethanol solution. The excitation wavelength was 410 nm.

The fluorescence spectra in Figure 28 – Figure 31 show intense emission ranges of dye extracts from roselle, turmeric, *Monascus* red and *Monascus* yellow at 380-730 (λ_{max} 455 nm), 440-700 (λ_{max} 520 nm), 475-760 (λ_{max} 545 nm) and 420-750 (λ_{max} 550 nm), respectively. The fluorescence spectrum of roselle extract shows additional less intense emission range at 740-900 nm. The fluorescence property of these dyes indicates the possibility of using them as sensitizers.

1.2.2 The fluorescence spectrum of [Ru(4,4'-dicarboxylic bipyridyl)₂(NCS)₂] or N3 dye in ethanol solution is shown in Figure 32. The emission range is 665 to 880 nm with maximum emission (λ_{max}) wavelength at 800 nm.

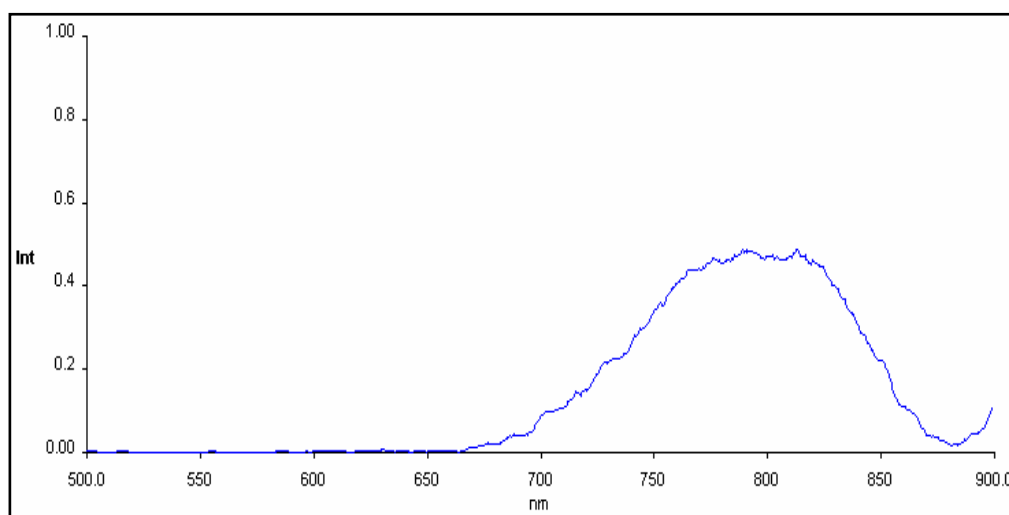


Figure 32 The fluorescence spectrum of N3 dye in ethanol solution. The excitation wavelength was 460 nm.

2. Electrochemical property of dyes extracted from roselle, turmeric, *Monascus* red and *Monascus* yellow rice culture and a ruthenium complex (N3) dye

2.1 The oxidation and reduction potentials of crude dyes extracted from roselle in ethanol solution were investigated by cyclic voltammetry at room temperature as shown in Figure 33 – Figure 34.

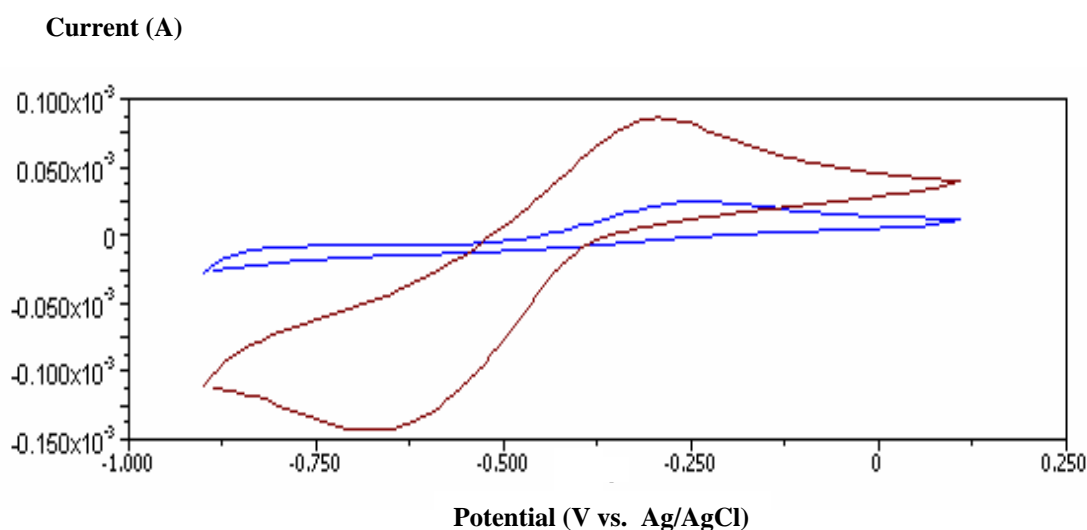


Figure 33 Cyclic voltammograms of roselle extract in aqueous solution containing 1M KNO_3 as supporting electrolyte (red line) and supporting electrolyte (blue line).

Cyclic voltammogram of roselle extract in ethanol solution containing 1 M KNO_3 as supporting electrolyte is shown in Figure 33. It was operated at scan rate of 100 mV/s from -0.9 to 0.1 V, working electrode was Pt electrode, auxiliary electrode was Pt wire and reference electrode was Ag/AgCl filled with saturated KCl. The quasi-reversible waves were observed with reduction wave at potential of -0.63 V and oxidation wave at potential of -0.31 V with reference to a Ag/AgCl electrode.

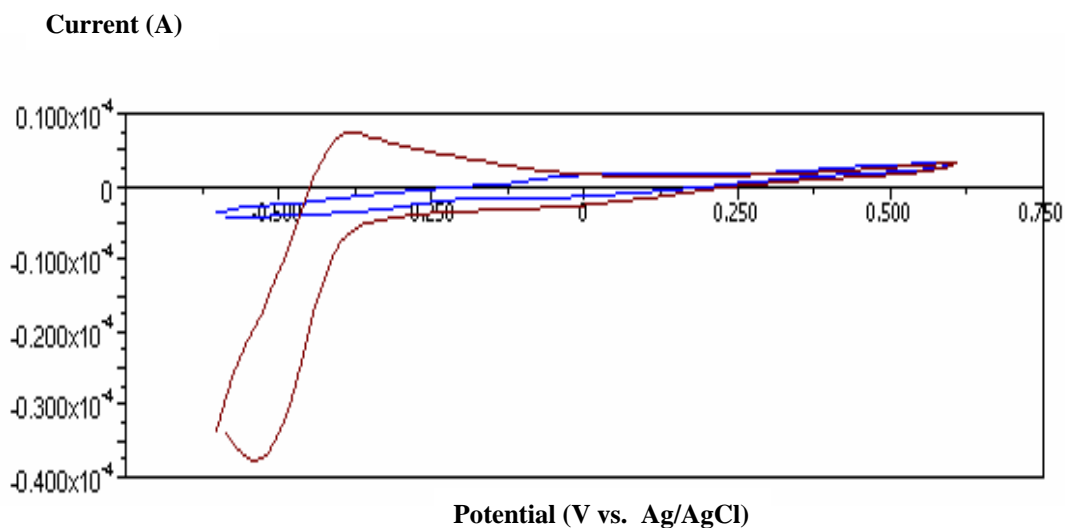


Figure 34 Cyclic voltammograms of roselle extract in aqueous solution containing 0.1 M Na₂SO₄ as supporting electrolyte (red line) and supporting electrolyte (blue line).

Cyclic voltammogram of roselle extract in ethanol solution containing 0.1 M Na₂SO₄ as supporting electrolyte is shown in Figure 34. It was operated at scan rate of 100 mV/s from -0.6 to 0.6 V, working electrode was Pt electrode, auxiliary electrode was Pt wire and reference electrode was Ag/AgCl filled with saturated KCl. The quasi-reversible waves were observed with reduction wave at potential of -0.52 V and oxidation wave at potential of -0.38 V with reference to a Ag/AgCl electrode.

2.2 The oxidation and reduction potentials of crude dyes extracted from turmeric in ethanol solution were investigated by cyclic voltammetry at room temperature as shown in Figure 35 – Figure 40.

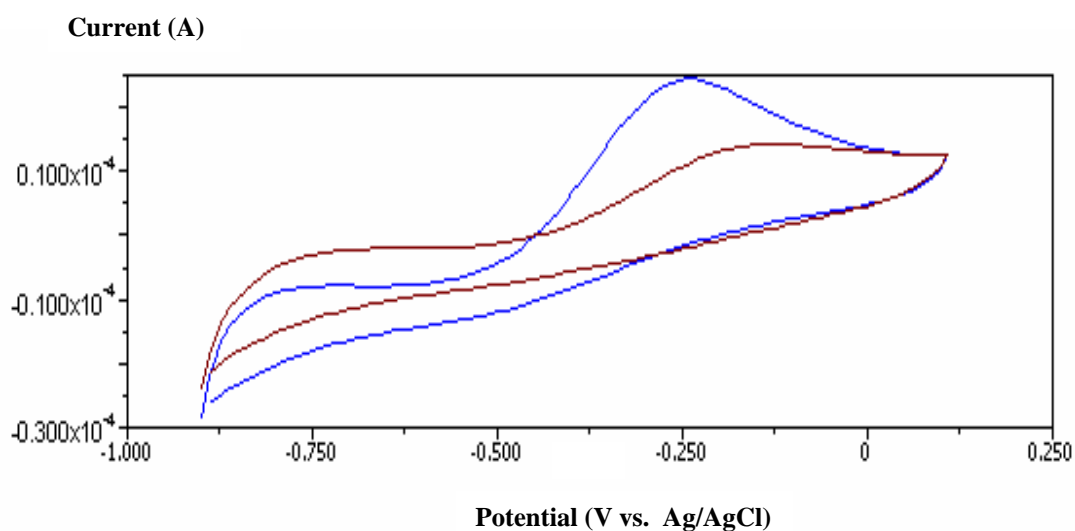


Figure 35 Cyclic voltammograms of turmeric extract in aqueous solution containing 1 M KNO_3 as supporting electrolyte (red line) and supporting electrolyte (blue line).

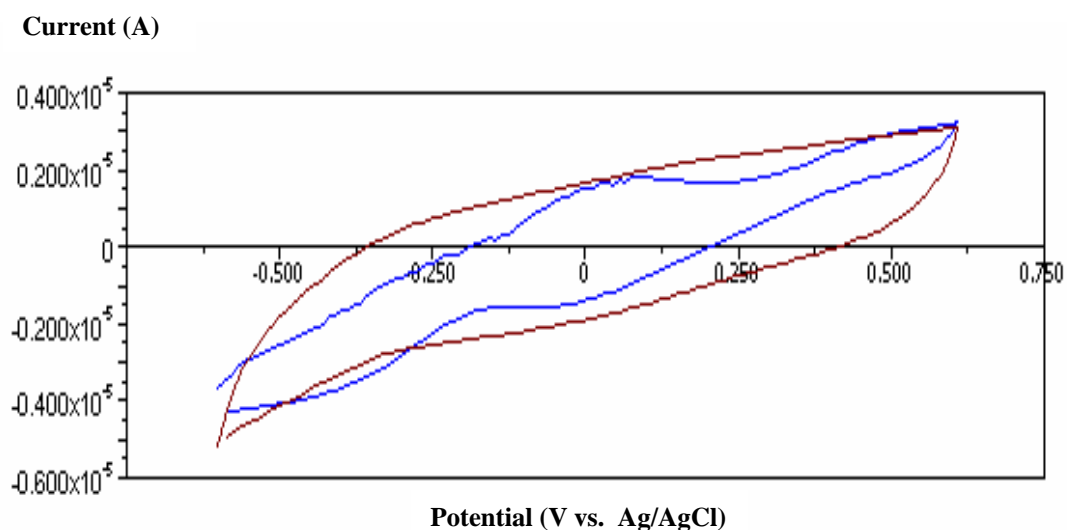


Figure 36 Cyclic voltammograms of turmeric extract in aqueous solution containing 0.1 M Na_2SO_4 as supporting electrolyte (red line) and supporting electrolyte (blue line).

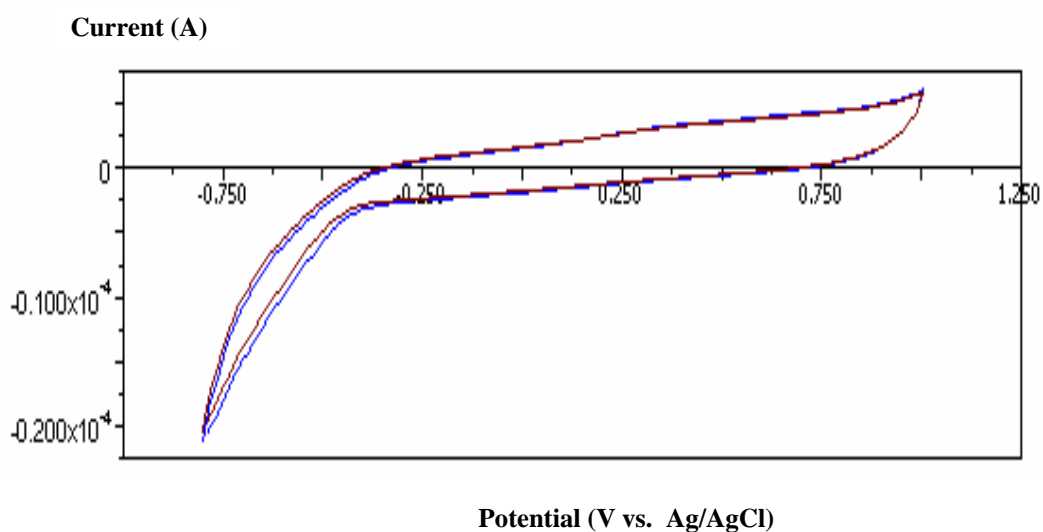


Figure 37 Cyclic voltammograms of turmeric extract in ethanol solution containing 0.1 M LiClO_4 as supporting electrolyte (red line) and supporting electrolyte (blue line).

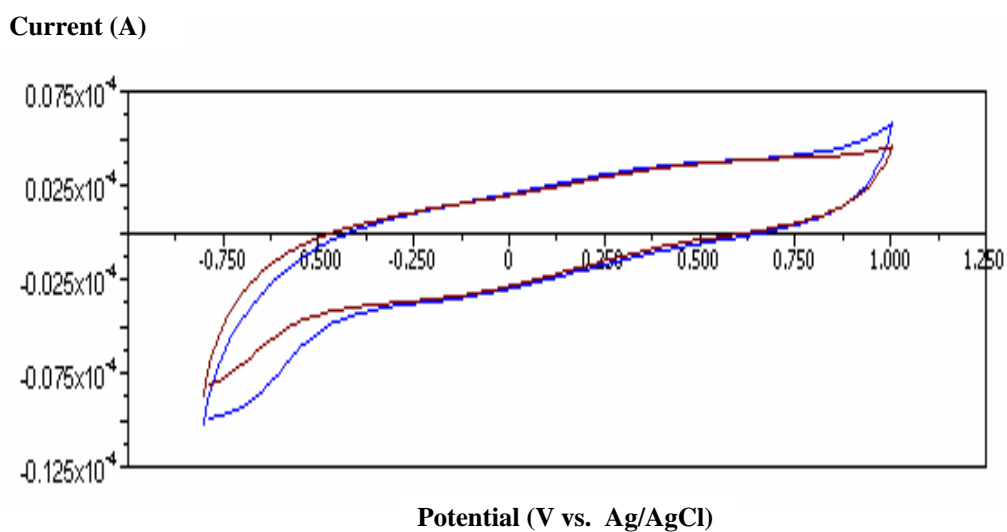


Figure 38 Cyclic voltammograms of turmeric extract in aqueous solution containing B-R buffer (pH 4) as supporting electrolyte (red line) and supporting electrolyte (blue line).

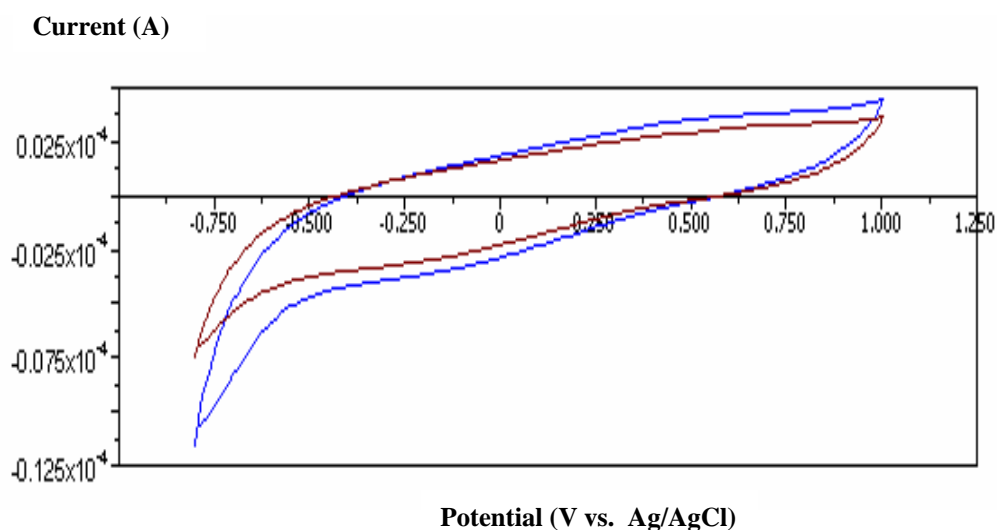


Figure 39 Cyclic voltammograms of turmeric extract in aqueous solution containing acetate buffer (pH 4) as supporting electrolyte (red line) and supporting electrolyte (blue line)

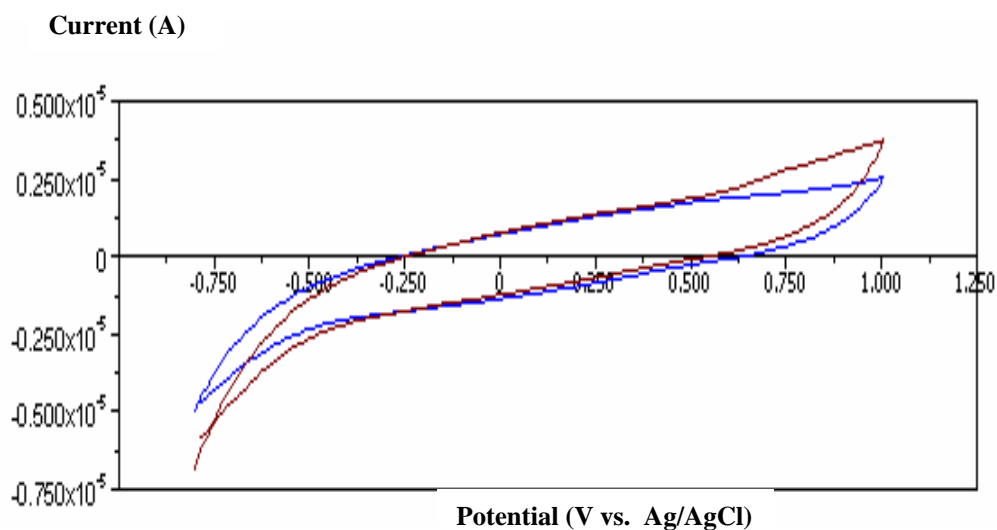


Figure 40 Cyclic voltammograms of turmeric extract in aqueous solution containing phosphate buffer (pH 3) as supporting electrolyte (red line) and supporting electrolyte (blue line).

From Figure 35 to Figure 40, the reduction and oxidation waves were not observed in the cyclic voltammograms of turmeric solution although various supporting electrolytes had been employed.

2.3 The oxidation and reduction potentials of crude dyes extracted from *Monascus* red in ethanol solution were investigated by cyclic voltammetry at room temperature as shown in Figure 41 – Figure 47.

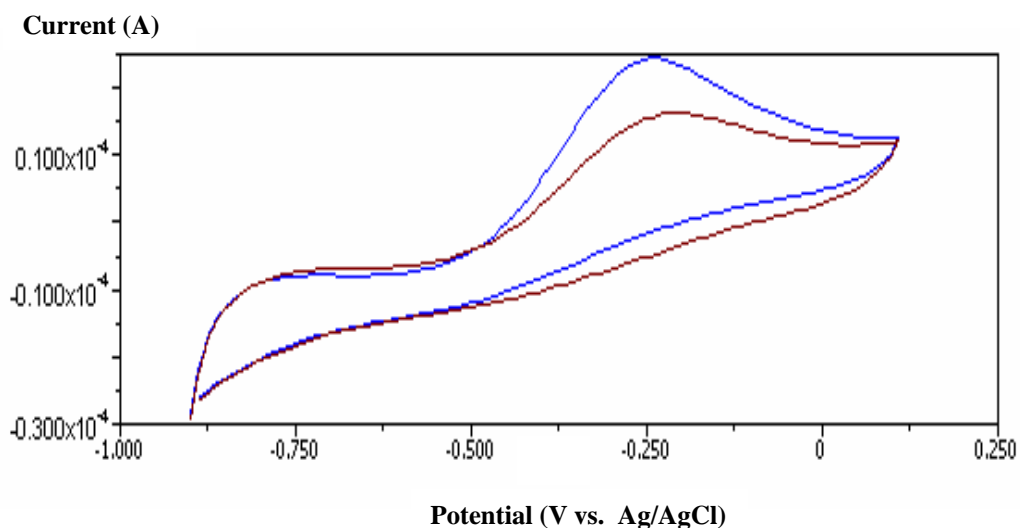


Figure 41 Cyclic voltammograms of *Monascus* red extract in aqueous solution containing 1 M KNO_3 as supporting electrolyte (red line) and supporting electrolyte (blue line).

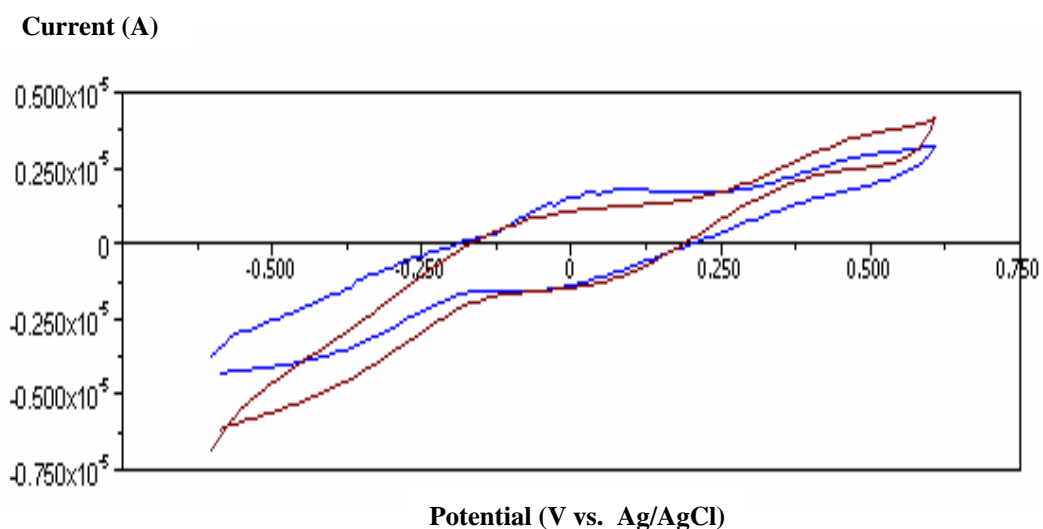


Figure 42 Cyclic voltammograms of *Monascus* red extract in aqueous solution containing 0.1 M Na_2SO_4 as supporting electrolyte (red line) and supporting electrolyte (blue line).

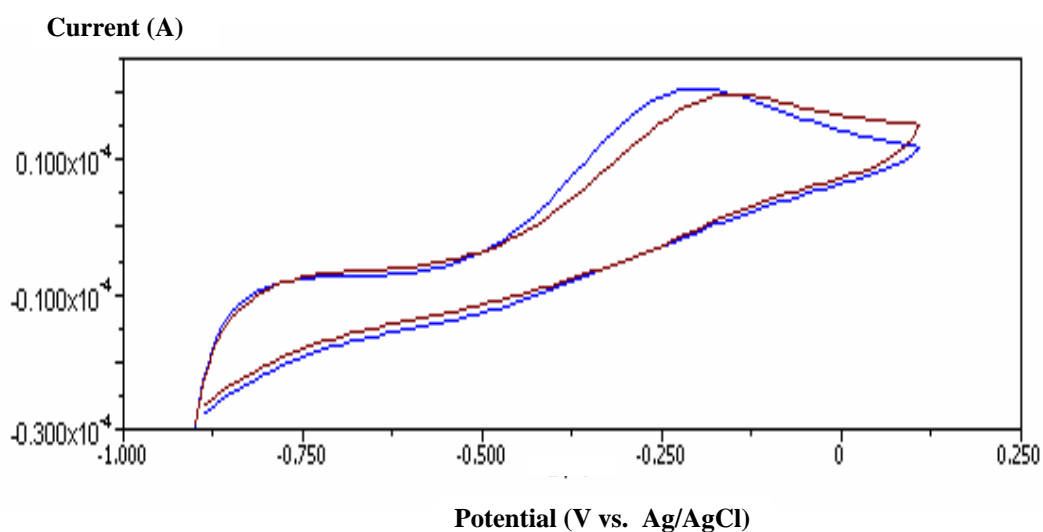


Figure 43 Cyclic voltammograms of *Monascus* red extract in aqueous solution containing 1 M KCl as supporting electrolyte (red line) and supporting electrolyte (blue line).

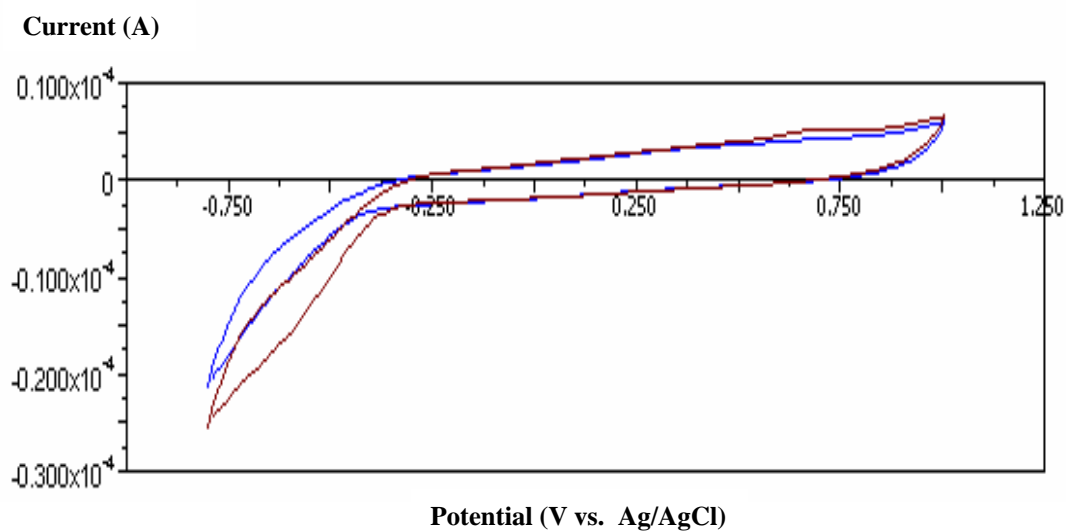


Figure 44 Cyclic voltammograms of *Monascus* red extract in ethanol solution containing 0.1 M LiClO_4 as supporting electrolyte (red line) and supporting electrolyte (blue line).

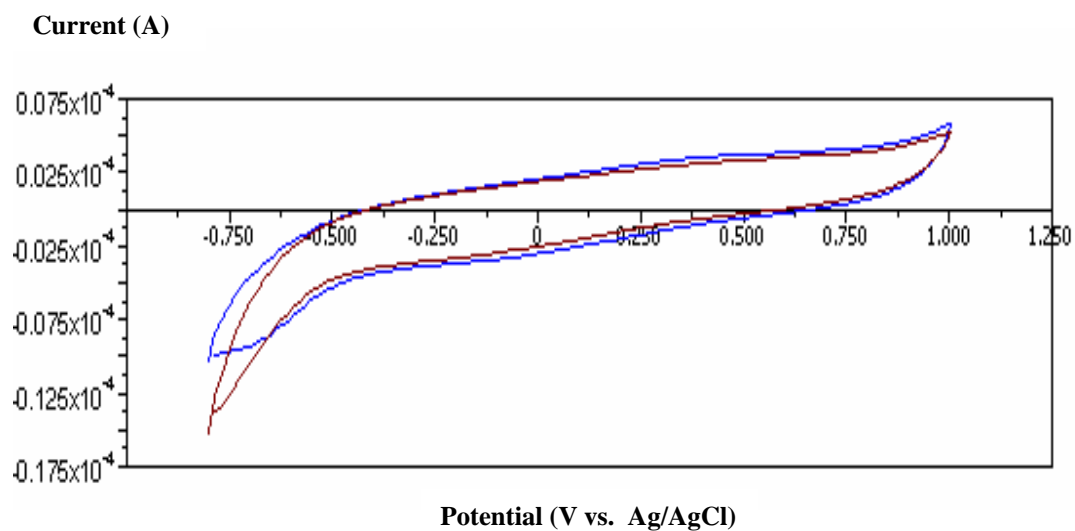


Figure 45 Cyclic voltammograms of *Monascus* red extract in aqueous solution containing B-R buffer (pH 4) as supporting electrolyte (red line) and supporting electrolyte (blue line).

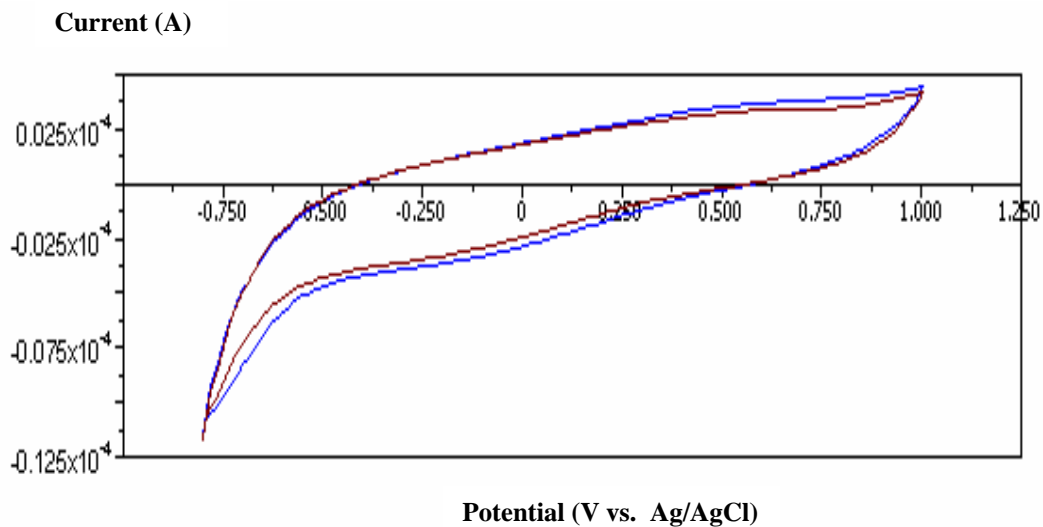


Figure 46 Cyclic voltammograms of *Monascus* red extract in aqueous solution containing acetate buffer (pH 4) as supporting electrolyte (red line) and supporting electrolyte (blue line).

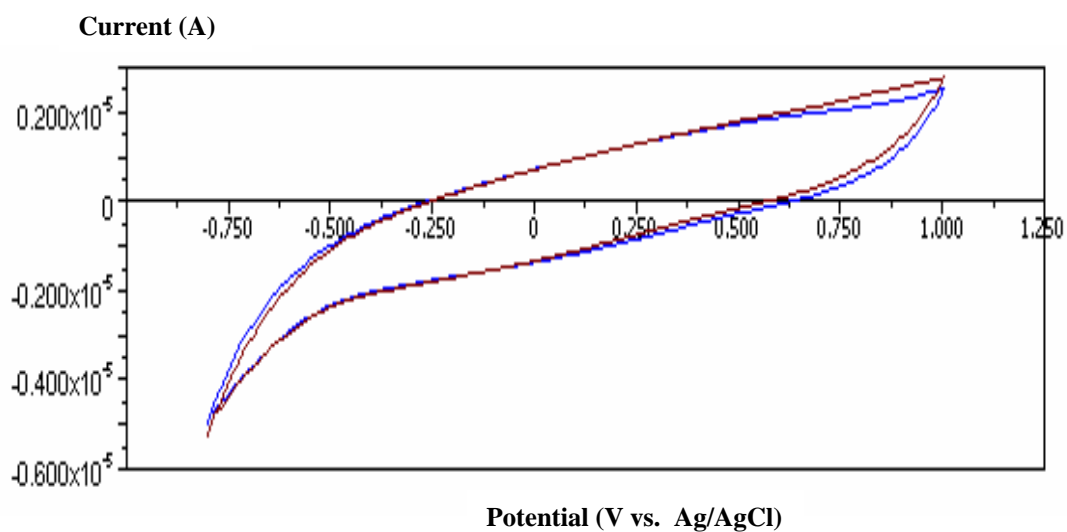


Figure 47 Cyclic voltammograms of *Monascus* red extract in aqueous solution containing phosphate buffer (pH 3) as supporting electrolyte (red line) and supporting electrolyte (blue line).

From Figure 41 to Figure 47, the reduction and oxidation waves were not observed in the cyclic voltammograms of *Monascus* red solution although various supporting electrolytes had been employed.

2.4 The oxidation and reduction potentials of crude dyes extracted from *Monascus* yellow in ethanol solution were investigated by cyclic voltammetry at room temperature as shown in Figure 48 – Figure 54.

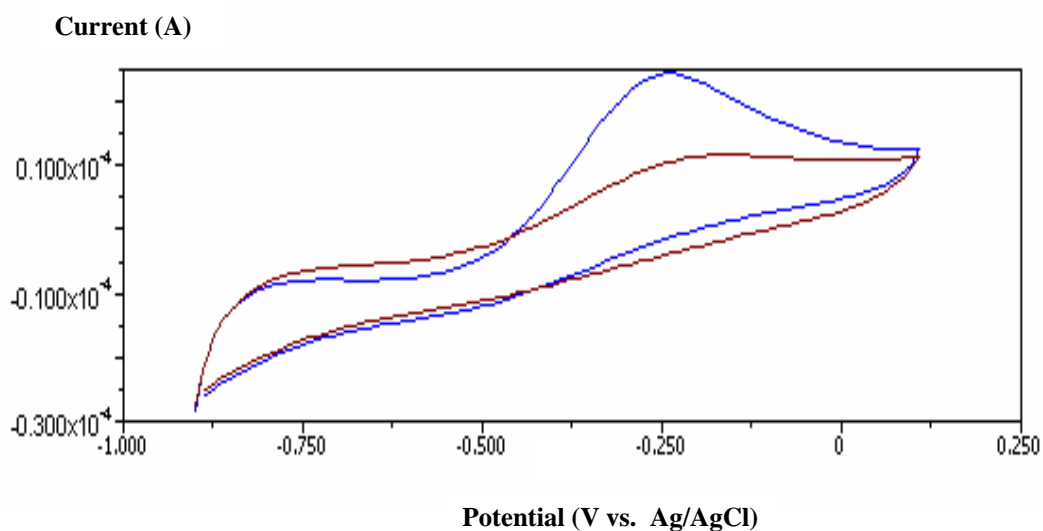


Figure 48 Cyclic voltammograms of *Monascus* yellow extract in aqueous solution containing 1 M KNO_3 as supporting electrolyte (red line) and supporting electrolyte (blue line) .

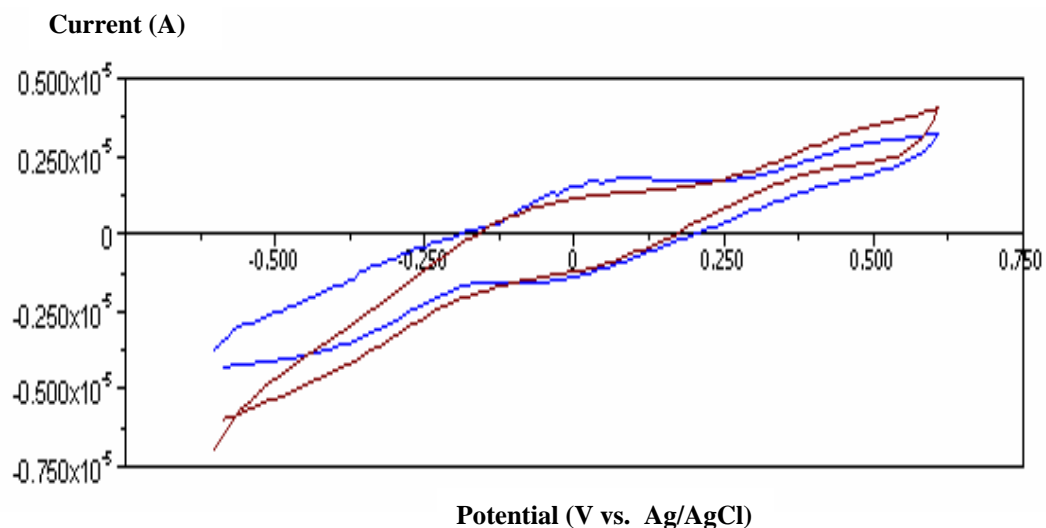


Figure 49 Cyclic voltammograms of *Monascus* yellow extract in aqueous solution containing 0.1 M Na_2SO_4 as supporting electrolyte (red line) and supporting electrolyte (blue line).

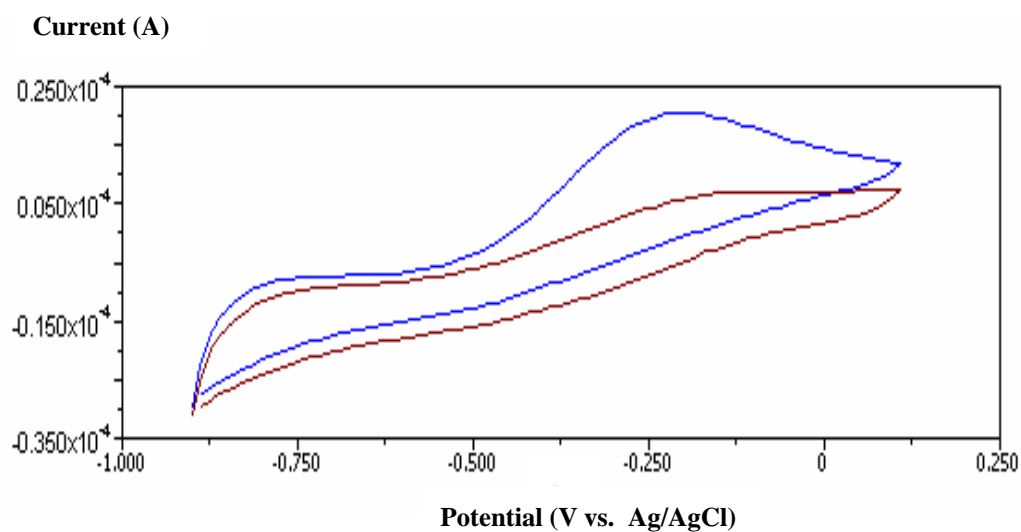


Figure 50 Cyclic voltammograms of *Monascus* yellow extract in aqueous solution containing 1 M KCl as supporting electrolyte (red line) and supporting electrolyte (blue line).

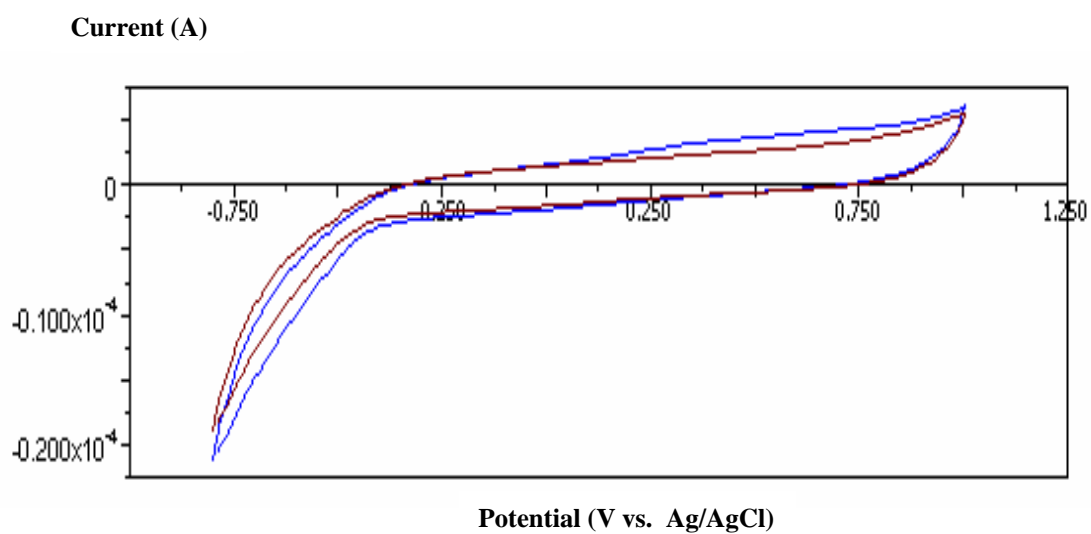


Figure 51 Cyclic voltammograms of *Monascus* yellow extract in ethanol solution containing 0.1 M LiClO_4 as supporting electrolyte (red line) and supporting electrolyte (blue line) .

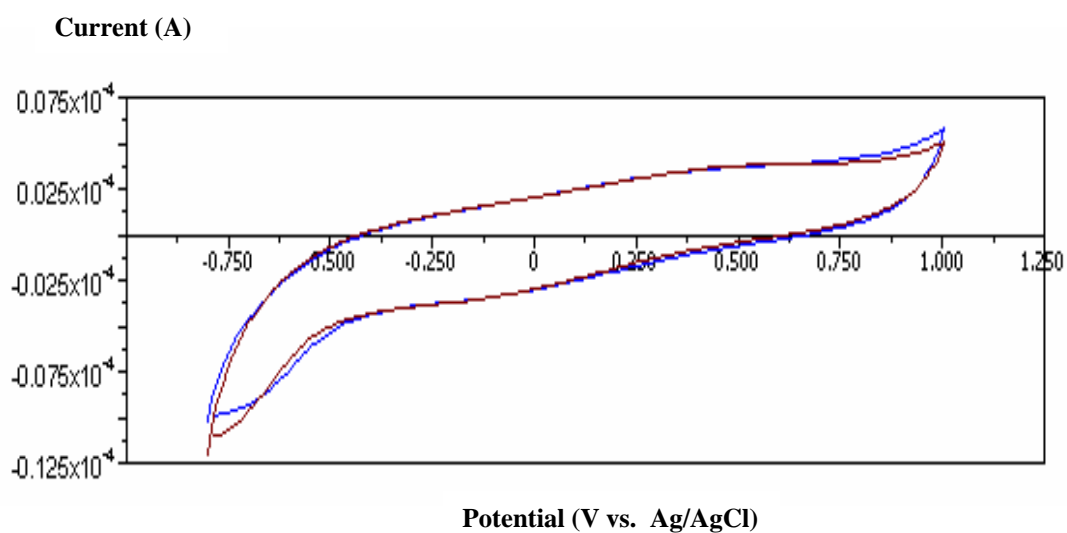


Figure 52 Cyclic voltammograms of *Monascus* yellow extract in aqueous solution containing B-R buffer (pH 4) as supporting electrolyte (red line) and supporting electrolyte (blue line).

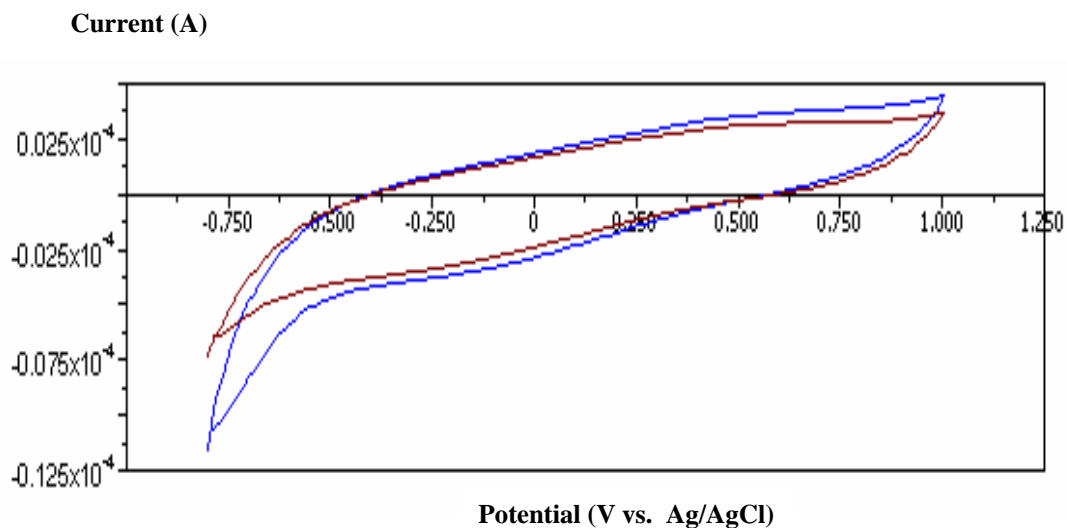


Figure 53 Cyclic voltammograms of *Monascus* yellow extract in aqueous solution containing acetate buffer (pH 4) as supporting electrolyte (red line) and supporting electrolyte (blue line).

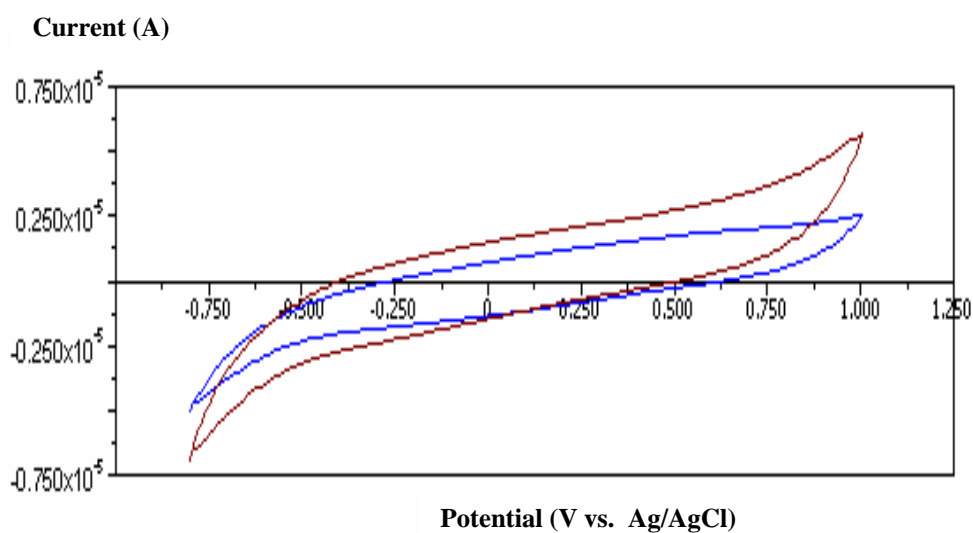


Figure 54 Cyclic voltammograms of *Monascus* yellow extract in aqueous solution containing phosphate buffer (pH 3) as supporting electrolyte (red line) and supporting electrolyte (blue line).

From Figure 48 to Figure 54, the reduction and oxidation waves were not observed in the cyclic voltammograms of *Monascus* yellow solution although various supporting electrolytes had been employed.

2.5 The oxidation and reduction potentials of crude mixed dye extracts in ethanol solution were investigated by cyclic voltammetry at room temperature as shown in Figure 55-60.

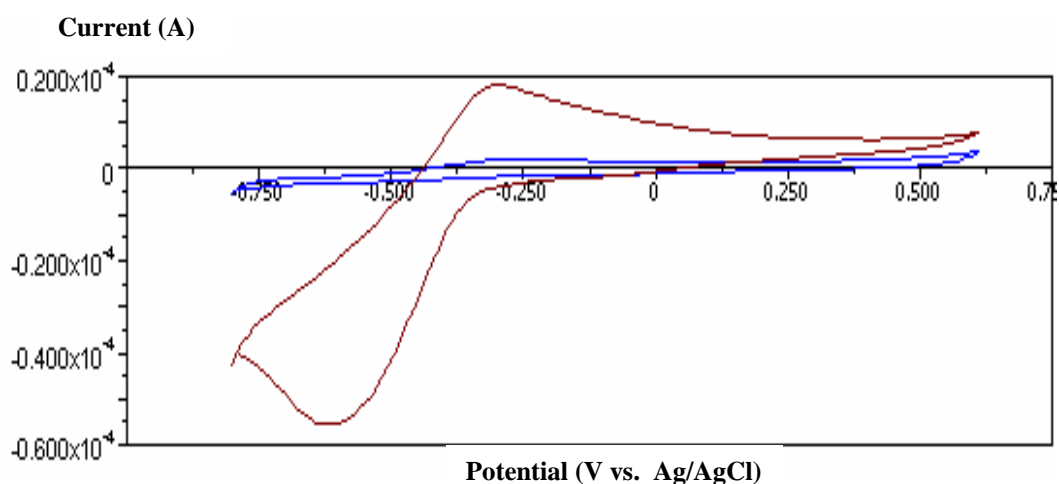


Figure 55 Cyclic voltammograms of mixture of roselle and turmeric extracts in aqueous solution containing 1 M KNO_3 as supporting electrolyte (red line) and supporting electrolyte (blue line).

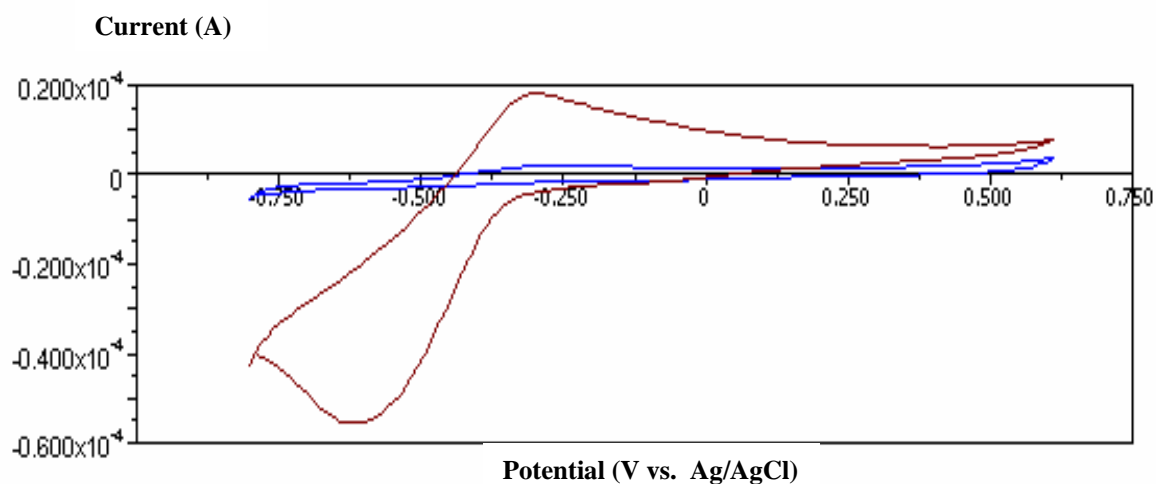


Figure 56 Cyclic voltammograms of mixture of roselle and *Monascus* red extracts in aqueous solution containing 1 M KNO_3 as supporting electrolyte (red line) and supporting electrolyte (blue line).

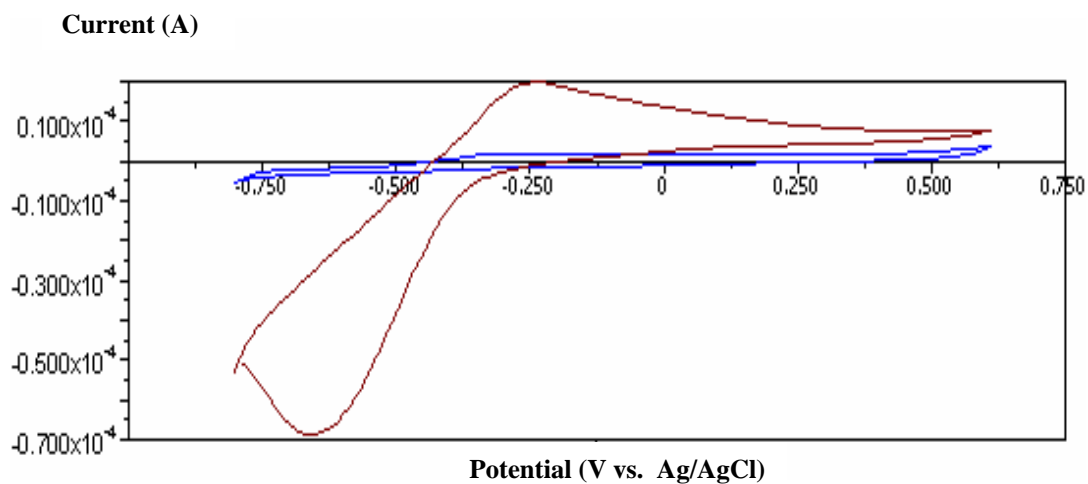


Figure 57 Cyclic voltammograms of mixture of roselle and *Monascus* yellow extracts in aqueous solution containing 1 M KNO_3 as supporting electrolyte (red line) and supporting electrolyte (blue line).

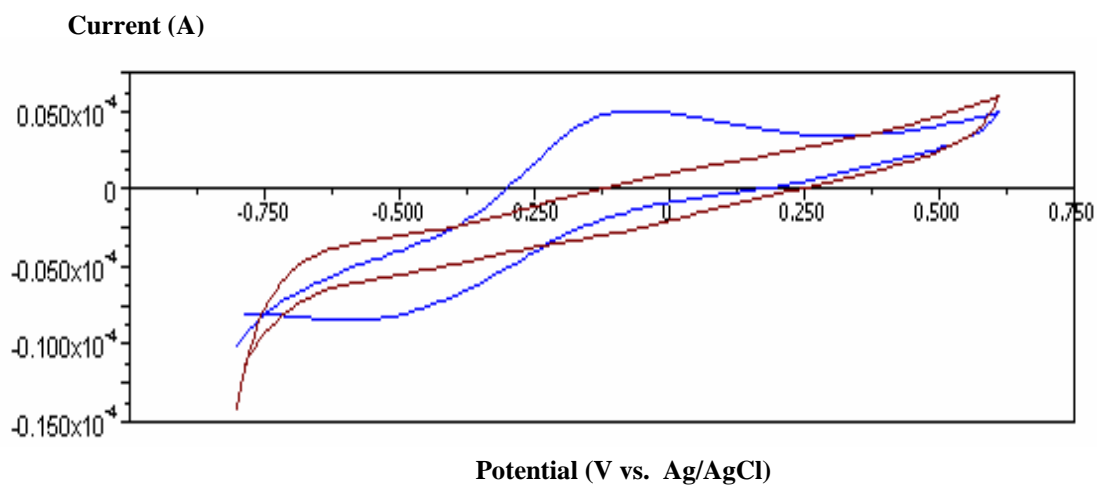


Figure 58 Cyclic voltammograms of mixture of turmeric and *Monascus* red extracts in aqueous solution containing 1 M KNO_3 as supporting electrolyte (red line) and supporting electrolyte (blue line).

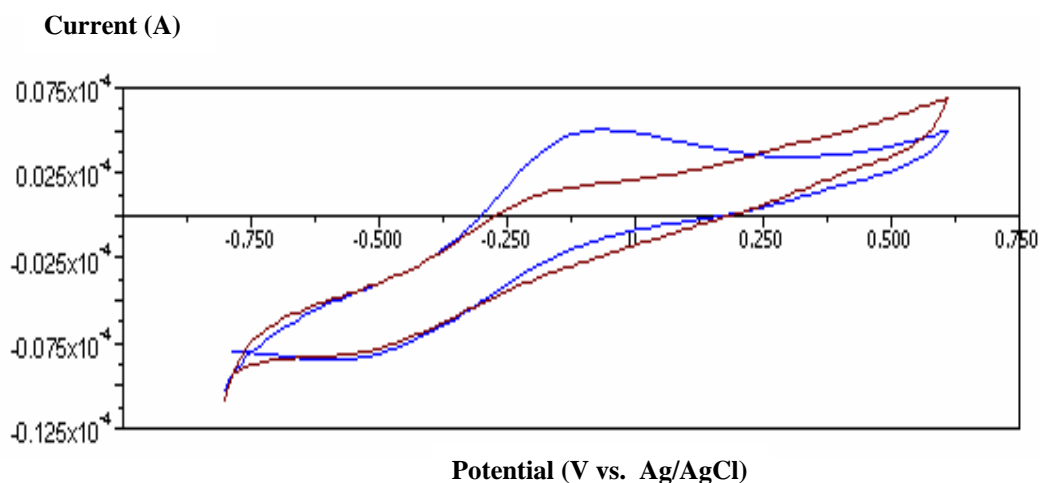


Figure 59 Cyclic voltammograms of mixture of turmeric and *Monascus* yellow extracts in aqueous solution containing 1 M KNO_3 as supporting electrolyte (red line) and supporting electrolyte (blue line).

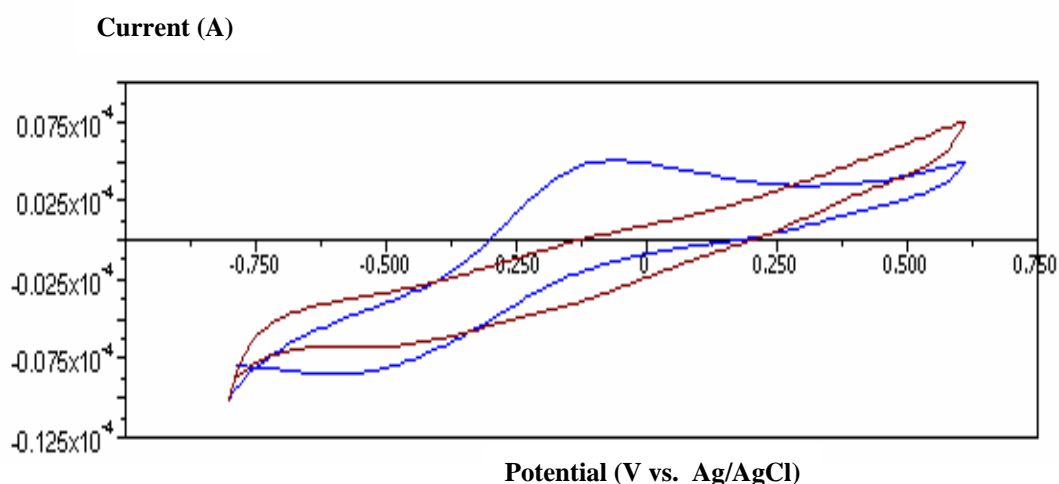


Figure 60 Cyclic voltammograms of mixture of *Monascus* red and *Monascus* yellow extracts in aqueous solution containing 1 M KNO_3 as supporting electrolyte (red line) and supporting electrolyte (blue line).

Cyclic voltammograms of mixed extracts containing roselle in ethanol solution containing 1 M KNO_3 as supporting electrolyte are shown in Figure 55 to Figure 57. These results showed that the cyclic voltammogram of mixed extracts containing roselle were similar to the cyclic voltammogram of roselle extract. Whereas the reduction and oxidation waves of other mixed extracts that shown in Figure 58 to Figure 60 were not observed in the cyclic voltammograms.

2.6 The oxidation and reduction potentials of $[\text{Ru}(4,4'\text{-dicarboxylic bipyridyl})_2(\text{NCS})_2]$ or N3 dye in ethanol solution were investigated by cyclic voltammetry at room temperature as shown in Figure 61.

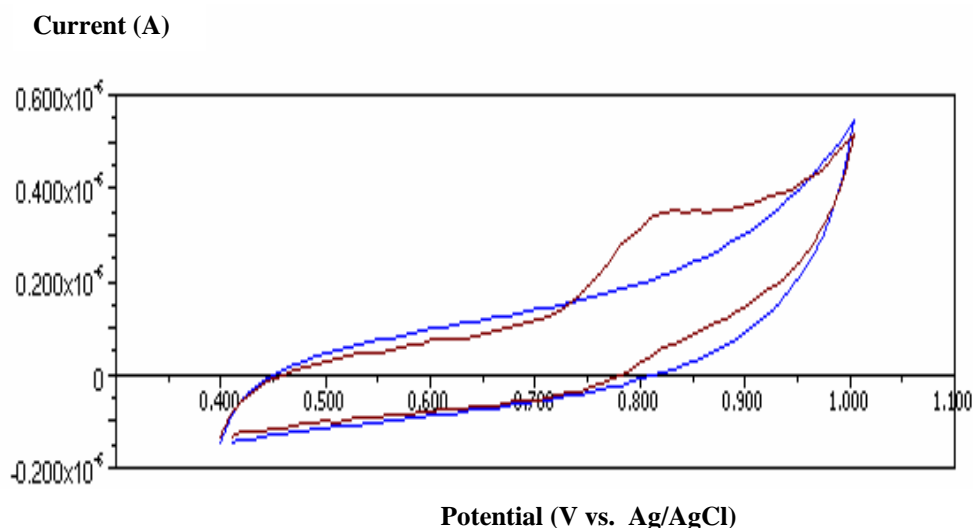


Figure 61 Cyclic voltammograms of $[\text{Ru}(4,4'\text{-dicarboxylic bipyridyl})_2(\text{NCS})_2]$ or N3 dye in ethanol solution containing 0.1 M LiClO_4 in ethanol solution as supporting electrolyte (red line) and supporting electrolyte (blue line).

Cyclic voltammogram of $[\text{Ru}(4,4'\text{-dicarboxylic bipyridyl})_2(\text{NCS})_2]$ or N3 dye in ethanol solution containing 0.1 M LiClO_4 in ethanol solution as supporting electrolyte is shown in Figure 61. It was scanned from 0.4 to 1.0 V with scan rate of 10 mV/s, working electrode was glassy carbon electrode, auxiliary electrode was Pt wire and reference electrode was Ag/AgCl filled with 0.1 M LiCl in methanol. The oxidation wave was observed at a potential of 0.813 V with reference to a Ag/AgCl electrode.

Generally inorganic elements possess redox properties because of large electronegativity difference between bonded elements (e.g. I_2/I^-). The heterocompounds (e.g. natural dye) and organo-metallic (e.g. N3 dye) like inorganic element also show redox property although they are covalent in nature. Therefore the dye extract, having redox property as well as light sensitivity, can be used in TiO_2 solar cells as a redox couple among the two where the other is I_2/I^- couple.

3. Effect of dye concentration on adsorption amount of dye on TiO₂ film

The amount of dye adsorbed on TiO₂ film was determined by spectroscopic measurement of the concentration change of the dye solution before and after adsorption.

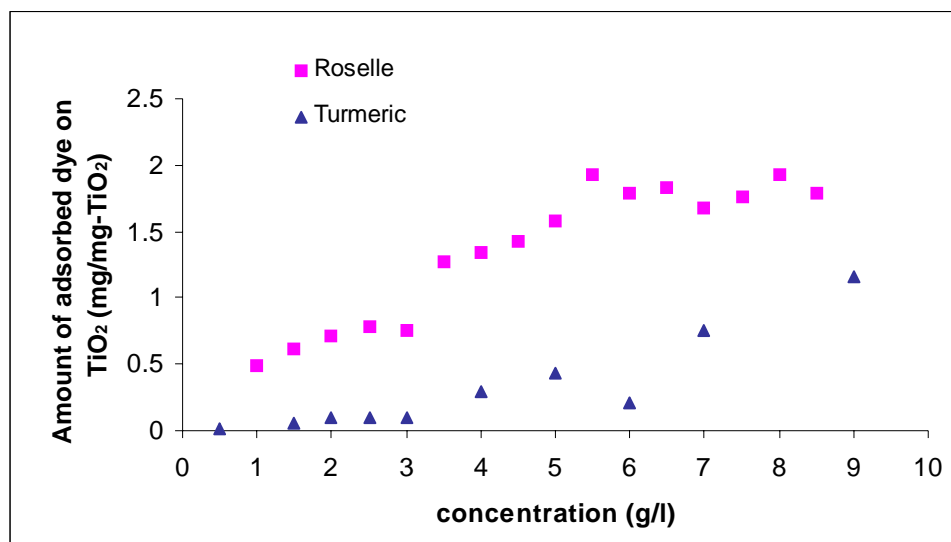


Figure 62 Amount of roselle and turmeric dye adsorbed on TiO₂ film on varying the dye concentration

The result in Figure 62 shows that as the concentrations of roselle and turmeric dyes were increased, the amounts of adsorbed dyes on TiO₂ film were increased. And the amount of adsorbed roselle dye on TiO₂ film are more than the amount of adsorbed turmeric dye on TiO₂ film at the same dye concentration due to the factor of molecular structure.

In addition, the relations between amount of adsorbed dye on TiO₂ film and concentration of roselle and turmeric dye extracts were studied by using Excel program to calculate the correlation coefficient, r and coefficient of determination, R^2 . These results showed r values as 0.925 and 0.911 and R^2 values as 0.8559 and 0.8300, respectively. They indicated that the amount of adsorbed dye on TiO₂ film and concentration of roselle and turmeric dye extracts were highly linear relation. The linear equations showing those relations were as below:

$$\text{Amount of adsorbed roselle dye} = 0.40 + 0.2(\text{concentration of roselle dye extract})$$

$$\text{Amount of adsorbed turmeric dye} = -0.19 + 0.1(\text{concentration of turmeric dye extract})$$

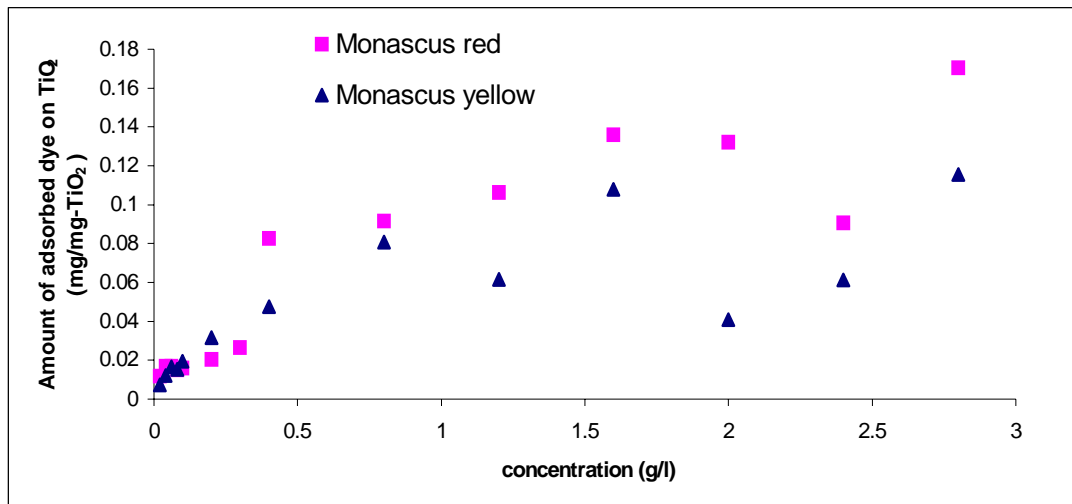


Figure 63 Amount of *Monascus* red and *Monascus* yellow adsorbed on TiO₂ film on varying the dye concentration

It can be seen from Figure 63 that as the concentrations of *Monascus* red and *Monascus* yellow were increased, the amounts of adsorbed dyes were increased however the concentration difference between before and after adsorption was so small that at high concentration of *Monascus* red and *Monascus* yellow, the small difference could be measured with less accuracy.

In addition, the relations between amount of adsorbed dye on TiO₂ film and concentration of *Monascus* red and *Monascus* yellow were studied by using Excel program to calculate the correlation coefficient, r and coefficient of determination, R^2 . These results showed r values as 0.897 and 0.780 and R^2 values as 0.8051 and 0.6081, respectively. They indicated that the amount of adsorbed dye on TiO₂ film and concentration of *Monascus* red and *Monascus* yellow were linear relation. The linear equations showing those relations were as below:

$$\text{Amount of adsorbed } \textit{Monascus} \text{ red} = 0.02 + 0.05(\text{concentration of } \textit{Monascus} \text{ red})$$

$$\text{Amount of adsorbed } \textit{Monascus} \text{ yellow} = 0.02 + 0.03(\text{concentration } \textit{Monascus} \text{ yellow})$$

Therefore the optimum concentrations for highest amounts of the adsorbed dyes were further investigated by observing optimum output of power (I_{sc} and V_{oc}) in the following experiments.

4. The current-voltage characteristics of the assembled dye-sensitized solar cells

4.1 The performance of TiO₂ solar cells sensitized with crude dyes extracted from plants and *Monascus* rice culture (batch 1) was monitored under an illuminator (3,000 K) with active area of cell of 1cm². All photoelectric parameters are shown in Table 1- Table 2.

Table 1 Photoelectrochemical parameters obtained from dye-sensitized solar cells assembled with liquid electrolyte (batch 1).

Dye	I_{sc} (mA)	V_{oc} (mV)	I_{mp} (mA)	V_{mp} (mV)	FF	%η
roselle 14.7030 g/l	0.0262	110	0.0123	60	0.2561	0.0015
Turmeric 4.4323 g/l	0.0406	90	0.0184	50	0.2518	0.0018
<i>Monascus</i> red 1.7021 g/l	0.0000	0.0000	0.0000	0.0000	0.0000	0.0000
<i>Monascus</i> yellow 5.2997 g/l	0.0054	15	0.0021	10	0.2593	0.0000
roselle : turmeric (3g :1g)	0.0815	245	0.0449	140	0.3148	0.0126
<i>Monascus</i> red : <i>Monascus</i> yellow (3g :1g)	0.0000	0.0000	0.0000	0.0000	0.0000	0.0000

$$P_{\text{light}} = 50 \text{ mWcm}^{-2}$$

Table 2 Photoelectrochemical parameters obtained from dye-sensitized solar cells assembled with solid polymer electrolyte (batch 1).

Dye	I_{sc} (mA)	V_{oc} (mV)	I_{mp} (mA)	V_{mp} (mV)	FF	%η
roselle 14.7030 g/l	0.1581	495	0.1247	340	0.5418	0.0848
turmeric 4.4323 g/l	0.009	165	0.0045	75	0.2273	0.0007
<i>Monascus</i> red 1.7021 g/l	0.0142	145	0.0071	75	0.2586	0.0011
<i>Monascus</i> yellow 5.2997 g/l	0.0433	415	0.0298	285	0.4726	0.0170
roselle : turmeric (3g :1g)	0.1623	425	0.0838	260	0.3159	0.0436
<i>Monascus</i> red: <i>Monascus</i> yellow (3g :1g)	0.0413	325	0.02	195	0.2906	0.0078

$$P_{\text{light}} = 50 \text{ mWcm}^{-2}$$

Generally, the dye-sensitized solar cells using the solid polymer electrolyte present lower conversion efficiency compared to the liquid electrolyte because of the incomplete wetting of the photoelectrode by the electrolyte. However, the results in Table 1 and Table 2 showed that the cells using liquid electrolyte present lower efficiency than those using solid electrode. This is due to the leakage of the liquid electrolyte and evaporation of solvent of the liquid electrolyte. Because of the sophisticated technique in sealing the cells and for the reason of long term stability of the electrolyte, solid polymer electrolyte were employed for the entire subsequent experiments.

4.2 The performance of dye-sensitized solar cells sensitized with Ru complex (N3) was monitored under an illuminator (3,000 K) with active area of cell of 1cm². All photoelectric parameters are shown in Table 3.

Table 3 Photoelectrochemical parameters obtained from dye-sensitized solar cells that sensitized with Ru complex (N3), using solid polymer electrolyte.

0.3 mM N3 sample batch	I_{sc} (mA)	V_{oc} (mV)	I_{mp} (mA)	V_{mp} (mV)	FF	%η
1 (batch 1)	0.8080	550	0.4260	280	0.2684	0.2386
2	1.4767	677	0.9925	397	0.3941	0.7880
3	0.3082	545	0.1703	325	0.3295	0.1107
	0.2477	690	0.1891	495	0.5477	0.1872
4	0.3993	565	0.2136	350	0.3314	0.1495
5 (batch 2)	0.2899	570	0.1456	280	0.2467	0.0815
	0.5200	720	0.3563	480	0.4568	0.3420
	0.3426	700	0.2137	470	0.4188	0.2009
6 (batch 3)	0.1582	630	0.0741	315	0.2342	0.0467
	0.2582	725	0.1569	460	0.3856	0.1443
	0.2778	740	0.1694	485	0.3997	0.1643

Table 3 (cont'd)

0.3 mM N3						
sample batch	I_{sc} (mA)	V_{oc} (mV)	I_{mp} (mA)	V_{mp} (mV)	FF	%η
7 (batch 4)						
	0.4386	620	0.2874	390	0.4122	0.2242
	0.5455	665	0.3147	400	0.3470	0.2518
	0.6615	570	0.4110	335	0.3652	0.2754
	0.6060	575	0.3798	350	0.3815	0.2659
	0.5341	585	0.3261	340	0.3549	0.2217
8 (batch 5)						
	1.0044	550	0.554	320	0.3209	0.3546
	1.0844	540	0.6190	295	0.3118	0.3652
	1.3405	550	0.7356	300	0.2993	0.4414

$$P_{\text{light}} = 50 \text{ mWcm}^{-2}$$

Table 3 presents the performance of dye-sensitized solar cell using Ru complex (N3) dye as sensitizer. The highest conversion efficiency (%η), short-circuit current (I_{sc}) and open-circuit voltage (V_{oc}) values were estimated to be 0.79%, 1.48 mA and 677 mV, respectively. The variation on the current and voltage values in each batch of sample occurs due to errors of the cells preparation such as variation of thickness of the TiO₂ film and platinum layer on the electrodes. And, the variation on the current and voltage values in the same cell occurs due to connection of the two electrodes from different site of the conducting glass. A connector at each electrode can be used to avoid this variation.

4.3 The performance of dye-sensitized solar cells sensitized with crude dyes extracted from plants and *Monascus* rice culture at various concentrations of dye solutions (batch 2, 3) was monitored under an illuminator (3,000 K) with active area of cell of 1cm². All photoelectric parameters are shown in Table 4 – Table 7.

4.3.1 The performance of dye-sensitized solar cells sensitized with crude dye extracted from roselle at various concentrations of dye solutions (batch 2, 3) was monitored under an illuminator (3,000 K) with active area of cell of 1cm². All photoelectric parameters are shown in Table 4.

Table 4 Photoelectrochemical parameters obtained from dye-sensitized solar cells that sensitized with roselle dye at various concentration of dye solutions (batch 2, 3), using solid polymer electrolyte

Concentration of roselle extract	I _{sc} (mA)	V _{oc} (mV)	I _{mp} (mA)	V _{mp} (mV)	FF	%η
3g/l (a)	0.1957	500	0.099	225	0.2276	0.0446
	0.1454	510	0.0931	335	0.4206	0.0624
3g/l (b)	0.2020	505	0.0989	240	0.2327	0.0475
	0.1957	505	0.1272	335	0.4312	0.0852
8g/l (b)	0.1880	505	0.0974	225	0.2308	0.0438
	0.1308	520	0.0918	340	0.4589	0.0624
12g/l (b)	0.2115	505	0.1026	230	0.2209	0.0472
	0.1333	520	0.0871	355	0.4461	0.0618
14g/l (a)	0.1818	510	0.0902	235	0.2286	0.0424
	0.2416	515	0.1567	340	0.4282	0.1066
16g/l (b)	0.2604	495	0.1568	285	0.3467	0.0894

(a) = batch 2 (b) = batch 3 P_{light} = 50 mWcm⁻²

Table 4 presents the performance of dye-sensitized solar cells sensitized with roselle of different concentrations of 3, 8, 12, 14 and 16 g/l. It can be seen that the effect of concentration of roselle dye solution in the range 3-16 g/l was not significant. Therefore, the concentration of 12 g/l of roselle dye solution was chosen for fabrication in the subsequent experiments.

4.3.2 The performance of dye-sensitized solar cells sensitized with crude dye extracted from turmeric at various concentrations of dye solutions (batch 2, 3) was monitored under an illuminator (3,000 K) with active area of cell of 1cm^2 . All photoelectric parameters are shown in Table 5.

Table 5 Photoelectrochemical parameters obtained from dye-sensitized solar cells that sensitized with turmeric dye at various concentration of dye solutions (batch 2, 3), using solid polymer electrolyte.

Concentration of turmeric extract	I_{sc} (mA)	V_{oc} (mV)	I_{mp} (mA)	V_{mp} (mV)	FF	$\% \eta$
3g/l	0.0955	465	0.0530	235	0.2805	0.0249
	0.1976	465	0.1170	280	0.3565	0.0655
	0.1585	465	0.0942	280	0.3579	0.0528
6g/l	0.0824	505	0.0451	265	0.2872	0.0239
	0.1475	480	0.0851	295	0.3546	0.0502
	0.1387	490	0.0797	295	0.3459	0.0470
12g/l	0.0592	470	0.0321	250	0.2884	0.0161
	0.1327	460	0.0807	290	0.3834	0.0468
	0.0985	465	0.0602	295	0.3877	0.0355

(a) = batch 2 (b) = batch 3 $P_{light} = 50 \text{ mWcm}^{-2}$

Table 5 presents the performance of dye-sensitized solar cells sensitized with turmeric of different concentrations of 3, 6 and 12g/l. It can be seen that the effect of concentration of turmeric dye solution in the range 3-12 g/l was not significant. Therefore, the concentration of 3 g/l of turmeric dye solution was chosen for fabrication in the subsequent experiments.

4.3.3 The performance of dye-sensitized solar cells sensitized with crude dye extracted from *Monascus* red rice culture at various concentrations of dye solutions (batch 2, 3) was monitored under an illuminator (3,000 K) with active area of cell of 1cm^2 . All photoelectric parameters are shown in Table 6.

Table 6 Photoelectrochemical parameters obtained from dye-sensitized solar cells that sensitized with *Monascus* red dye at various concentration of dye solutions (batch 2, 3), using solid polymer electrolyte.

Concentration of <i>Monascus</i> red extract	I_{sc} (mA)	V_{oc} (mV)	I_{mp} (mA)	V_{mp} (mV)	FF	$\% \eta$
1g/l (a)	0.0311	380	0.0199	245	0.4125	0.0098
	0.0166	345	0.0100	230	0.4016	0.0046
3g/l (a)	0.0754	425	0.0494	260	0.4008	0.0257
	0.0168	350	0.0104	230	0.4068	0.0048
8g/l (a)	0.1160	445	0.0714	240	0.3320	0.0343
	0.0454	435	0.0297	280	0.4211	0.0166
8g/l (b)	0.0449	485	0.0227	265	0.2762	0.0120
	0.0432	425	0.0283	280	0.4316	0.0158
12g/l (b)	0.0954	445	0.0507	225	0.2687	0.0228
	0.0437	410	0.0302	280	0.472	0.0169
16g/l (b)	0.0966	455	0.0482	210	0.2303	0.0202
	0.0283	405	0.0198	285	0.4923	0.0113

(a) = batch 2 (b) = batch 3 $P_{light} = 50\text{ mWcm}^{-2}$

Table 6 presents the performance of dye-sensitized solar cells sensitized with *Monascus* red of different concentrations of 1, 3, 8, 12 and 16 g/l. It can be seen that the effect of concentration of *Monascus* red dye solution in the range 1-16 g/l was not significant. Therefore the concentration of 8 g/l of *Monascus* red dye solution was chosen for fabrication in the subsequent experiments.

4.3.4 The performance of dye-sensitized solar cells sensitized with crude dye extracted from *Monascus* yellow rice culture at various concentrations of dye solutions (batch 2, 3) was monitored under an illuminator (3,000 K) with active area of cell of 1cm^2 . All photoelectric parameters are shown in Table 7.

Table 7 Photoelectrochemical parameters obtained from dye-sensitized solar cells that sensitized with *Monascus* yellow dye at various concentration of dye solutions (batch 2, 3), using solid polymer electrolyte.

Concentration of <i>Monascus</i> yellow extract	I_{sc} (mA)	V_{oc} (mV)	I_{mp} (mA)	V_{mp} (mV)	FF	% η
3g/l (a)	0.0745	440	0.0456	240	0.3339	0.0219
	0.0287	375	0.0185	260	0.4469	0.0096
10g/l (a)	0.1954	455	0.1324	295	0.4393	0.0781
	0.0211	365	0.0154	250	0.4999	0.0077
10g/l (b)	0.1391	485	0.0706	185	0.1936	0.0261
	0.0764	440	0.0503	285	0.4264	0.0287
12g/l (b)	0.1015	460	0.0557	215	0.2565	0.024
	0.053	415	0.0368	289	0.4835	0.0213
16g/l (a)	0.0576	480	0.0342	245	0.3031	0.0168
	0.0623	435	0.0388	280	0.4009	0.0217
16g/l (b)	0.0862	460	0.0476	220	0.2641	0.0209
	0.0324	305	0.0208	175	0.3683	0.0073

(a) = batch 2 (b) = batch 3 $P_{light} = 50 \text{ mWcm}^{-2}$

Table 7 presents the performance of dye-sensitized solar cells sensitized with *Monascus* yellow of different concentrations of 3, 10, 12 and 16 g/l. It can be seen that the effect of concentration of *Monascus* yellow dye solution in the range 3-16 g/l was not significant. Therefore the concentration of 10 g/l of *Monascus* yellow dye solution was chosen for fabrication in the subsequent experiments.

4.4 The performance of dye-sensitized solar cells sensitized with mixture of crude dyes extracted from plants and *Monascus* rice culture at concentration of dye solutions of 6 g/l (batch 2) was monitored under an illuminator (3,000 K, $P_{\text{light}} = 50 \text{ mWcm}^{-2}$) with active area of cell of 1cm^2 . All photoelectric parameters are shown in Table 8.

Table 8 Photoelectrochemical parameters obtained from dye-sensitized solar cells that sensitized with mixture dyes (batch 2) and using solid polymer electrolyte

Mixture of dyes	I_{sc} (mA)	V_{oc} (mV)	I_{mp} (mA)	V_{mp} (mV)	FF	% η
roselle:turmeric	0.1420	515	0.0701	215	0.2061	0.0301
	0.1468	530	0.0887	325	0.3705	0.0577
roselle/turmeric	0.0674	525	0.0404	285	0.3254	0.0230
	0.0572	485	0.0352	325	0.4124	0.0229
turmeric/roselle	0.1408	490	0.0681	205	0.2023	0.0279
	0.2082	515	0.1198	305	0.3408	0.0731
<i>Monascus</i> red: <i>Monascus</i> yellow	0.0580	460	0.0335	250	0.3139	0.0168
	0.0573	435	0.0359	285	0.4105	0.0205
	0.0429	435	0.0275	285	0.4200	0.0157
<i>Monascus</i> red / <i>Monascus</i> yellow	0.0916	455	0.0567	250	0.3401	0.0284
	0.0447	420	0.0303	280	0.4519	0.0170
<i>Monascus</i> yellow/ <i>Monascus</i> red	0.0811	450	0.0498	250	0.3411	0.0249
	0.0444	420	0.0283	280	0.4249	0.0158

The results from Table 8 showed that the performance of dye-sensitized solar cells sensitized with mixed dyes of roselle and turmeric on impregnating roselle dye after the impregnation of turmeric was better than that with different order of impregnation of the two dyes, but was not much different from the one with mixed solution of the two dyes. This might be due to the better sensitization property and better adsorption on TiO_2 particles of roselle dye than turmeric dye. Therefore the subsequent experiments were performed with mixed solution of the two dyes.

The performance of dye-sensitized with mixed dyes of *Monascus* red and *Monascus* yellow showed not much difference on impregnation of dyes with two different methods, therefore the subsequent experiments were performed with mixed solution of the two dyes.

4.5 The performance of dye-sensitized solar cells sensitized with crude dyes extracted from plants and *Monascus* rice culture and mixed dye (batch 4, 5) was monitored under an illuminator (3,000 K, $P_{\text{light}} = 50 \text{ mWcm}^{-2}$) with active area of cell of 1cm^2 . All photoelectric parameters are shown in Table 9 and Table 10.

Table 9 Photoelectrochemical parameters obtained from dye-sensitized solar cells that sensitized with crude dyes extracted from plants and *Monascus* rice cultures and mixed dyes (batch 4), using solid polymer electrolyte

Dye	I_{sc} (mA)	V_{oc} (mV)	I_{mp} (mA)	V_{mp} (mV)	FF	$\% \eta$
roselle 12 g/l						
	0.2875	455	0.1865	285	0.4063	0.1063
	0.3002	445	0.2022	280	0.4238	0.1132
	0.2736	460	0.1866	295	0.4374	0.1101
average	0.2871	453	0.1918	287	0.4225	0.1099
turmeric 3 g/l						
	0.0611	420	0.0388	280	0.4233	0.0217
	0.0639	415	0.0395	275	0.4096	0.0217
	0.0681	415	0.0430	270	0.4108	0.0232
average	0.0644	417	0.0404	275	0.4146	0.0222
<i>Monascus</i> red 8 g/l						
	0.0658	420	0.0433	270	0.423	0.0234
	0.0518	395	0.0339	270	0.4473	0.0183
	0.0612	395	0.0409	265	0.4484	0.0217
average	0.0596	403	0.0394	268	0.4396	0.0211
<i>Monascus</i> yellow 10 g/l						
	0.0542	440	0.0350	280	0.4109	0.0196
	0.0462	425	0.0306	280	0.4364	0.0171
	0.0535	425	0.0352	280	0.4335	0.0197
average	0.0513	438	0.0336	280	0.4269	0.0188

Table 9 (cont'd)

Dye	I_{sc} (mA)	V_{oc} (mV)	I_{mp} (mA)	V_{mp} (mV)	FF	%η
roselle : turmeric (650g : 1g)						
	0.1772	470	0.1032	295	0.3655	0.0609
	0.1914	455	0.1150	285	0.3763	0.0656
	0.1819	450	0.1180	290	0.4181	0.0684
average	0.1835	458	0.1121	290	0.3866	0.0650
roselle : <i>Monascus</i> red (112g : 1g)						
	0.2260	475	0.1477	265	0.3646	0.0783
	0.1907	460	0.1314	280	0.4194	0.0736
	0.1185	445	0.0864	290	0.4752	0.0501
average	0.1784	460	0.1218	278	0.4197	0.0673
roselle : <i>Monascus</i> yellow (56g : 1g)						
	0.4898	470	0.3252	275	0.3885	0.1789
	0.5257	465	0.3554	275	0.3998	0.1955
	0.4546	460	0.3073	270	0.3968	0.1659
average	0.4900	465	0.3293	273	0.3950	0.1801
turmeric : <i>Monascus</i> red (1g : 6g)						
	0.0587	445	0.0393	290	0.4363	0.0228
	0.0627	440	0.0401	300	0.4361	0.0241
	0.0575	435	0.0372	290	0.4313	0.0216
average	0.0596	440	0.0389	293	0.4346	0.0228
turmeric : <i>Monascus</i> yellow (1g : 12g)						
	0.0626	440	0.0423	290	0.4454	0.0245
	0.0647	430	0.0430	295	0.456	0.0254
	0.0585	420	0.0396	290	0.4674	0.0230
average	0.0619	430	0.0416	292	0.4563	0.0243
<i>Monascus</i> red : <i>Monascus</i> yellow (1g : 2g)						
	0.0625	425	0.0427	305	0.4903	0.0260
	0.0586	425	0.0410	305	0.5021	0.0250
	0.0618	425	0.0428	305	0.4970	0.0261
average	0.0610	425	0.0422	305	0.4965	0.0257

Table 10 Photoelectrochemical parameters obtained from dye-sensitized solar cells that sensitized with crude dyes extracted from plants and *Monascus* rice cultures and mixed dyes (batch 5), using solid polymer electrolyte

Dye	I_{sc} (mA)	V_{oc} (mV)	I_{mp} (mA)	V_{mp} (mV)	FF	%η
roselle 12 g/l						
	0.9406	465	0.5960	250	0.3407	0.2980
	0.8920	465	0.5787	255	0.3558	0.2951
	0.9789	470	0.6496	260	0.3671	0.3378
average	0.9372	467	0.6081	255	0.3545	0.3236
turmeric 3 g/l						
	0.2837	445	0.1780	280	0.3948	0.0997
	0.3111	455	0.1939	280	0.3836	0.1086
	0.3043	460	0.1849	270	0.3566	0.0998
average	0.2997	453	0.1856	277	0.3783	0.1027
<i>Monascus</i> red 8 g/l						
	0.3013	415	0.2104	265	0.4459	0.1115
	0.2734	415	0.2005	280	0.4948	0.1123
	0.2244	420	0.1646	290	0.5065	0.0955
average	0.2664	417	0.1918	278	0.4824	0.1064
<i>Monascus</i> yellow 10 g/l						
	0.2793	430	0.1978	270	0.4447	0.1068
	0.2674	430	0.2002	290	0.5049	0.1161
	0.2698	440	0.2000	285	0.4802	0.1140
average	0.2722	433	0.1993	282	0.4766	0.1123
roselle : turmeric (650g : 1g)						
	0.7500	470	0.4679	260	0.3451	0.2433
	0.7269	465	0.4895	270	0.3910	0.2643
	0.7128	460	0.4830	270	0.3977	0.2608
average	0.7299	465	0.4801	267	0.3779	0.2561

Table 10 (cont'd)

Dye	I _{sc} (mA)	V _{oc} (mV)	I _{mp} (mA)	V _{mp} (mV)	FF	%η
roselle : <i>Monascus</i> red (112g : 1g)						
	0.6605	455	0.4800	280	0.4472	0.2688
	0.6929	465	0.4795	275	0.4093	0.2637
	0.6868	445	0.4901	255	0.4089	0.2500
average	0.6801	455	0.4832	270	0.4218	0.2608
roselle : <i>Monascus</i> yellow (56g : 1g)						
	0.5101	485	0.3420	305	0.4216	0.2086
	0.5089	490	0.3445	310	0.4283	0.2136
	0.4863	485	0.3318	300	0.4220	0.1991
average	0.5018	487	0.3394	305	0.4240	0.2071
turmeric : <i>Monascus</i> red (1g : 6g)						
	0.2864	450	0.1961	290	0.4413	0.1137
	0.2911	440	0.2059	290	0.4662	0.1194
	0.2778	440	0.1951	285	0.4549	0.1112
average	0.2851	443	0.1990	288	0.4541	0.1148
turmeric : <i>Monascus</i> yellow (1g : 12g)						
	0.2568	470	0.1775	315	0.4633	0.1118
	0.2356	455	0.1672	315	0.4913	0.1053
	0.2374	455	0.1676	310	0.4810	0.1039
average	0.2433	460	0.1708	313	0.4785	0.1070
<i>Monascus</i> red : <i>Monascus</i> yellow (1g : 2g)						
	0.1274	445	0.0934	310	0.5107	0.0579
	0.1363	445	0.0968	330	0.5267	0.0639
	0.1341	445	0.0975	325	0.5310	0.0634
average	0.1326	445	0.0959	322	0.5288	0.0617

$$P_{\text{light}} = 50 \text{ mWcm}^{-2}$$

The results from Table 9 and Table 10 were performed from dye-sensitized solar cells fabricated with similar conditions except that solid electrolyte used to fabricate dye-sensitized solar cells for Table 10 was freshly prepared before use while those for Table 9 was 3 weeks olds. This resulted in better performance of dye-sensitized solar cells shown in Table 10 than those in Table 9.

From the results in Table 10, it can be seen that roselle dye is the best sensitizer of the four natural dyes studied. The conversion efficiency ($\% \eta$), short-circuit current (I_{sc}) and open-circuit current (V_{oc}) were 0.32%, 0.94 mAcm^{-2} and 467 mV, respectively.

The turmeric dye and *Monascus* red and *Monascus* yellow pigments showed similar sensitizing effect. The conversion efficiency ($\% \eta$), short-circuit current (I_{sc}) and open-circuit current (V_{oc}) were 0.10, 0.11, 0.11 %, 0.30, 0.27, 0.27 mAcm^{-2} and 453, 417, 433 mV, respectively.

The performances of the solar cells sensitized with mixed dyes with roselle as one of the combination were better than those sensitized with turmeric, *Monascus* red and *Monascus* yellow alone but were less than that sensitized with roselle alone due to the most effective sensitizer of roselle dye.

4.6 The Current-voltage (I-V) curves of dye-sensitized solar cell sensitized with crude dyes extracted from plants and *Monascus* rice culture and mixture of dyes (batch 5) that monitored under an illuminator (3,000 K) with active area of cell of 1cm^2 are shown in Figure 64-Figure 73

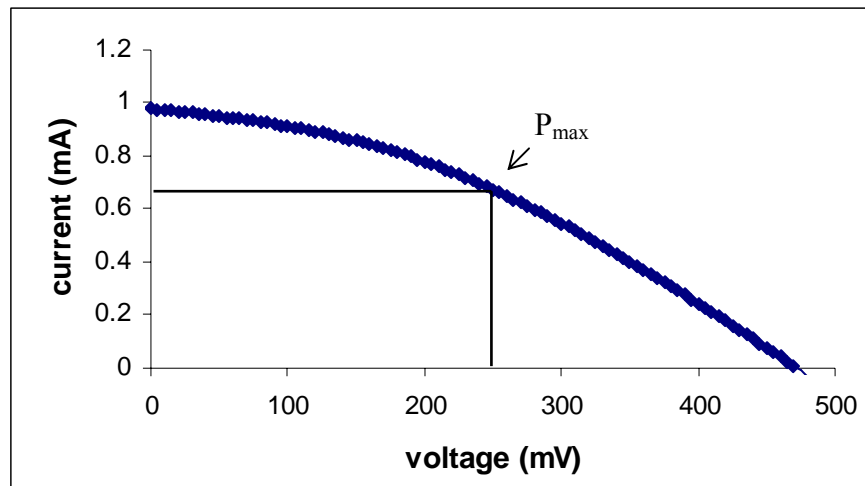


Figure 64 Current-voltage (I-V) curve of dye-sensitized solar cell that sensitized with roselle dye, using solid polymer electrolyte.

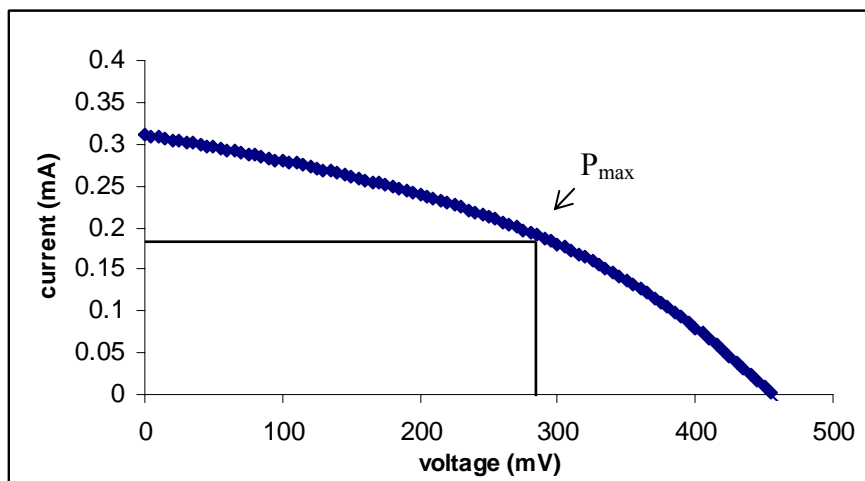


Figure 65 Current-voltage (I-V) curve of dye-sensitized solar cell that sensitized with turmeric dye, using solid polymer electrolyte

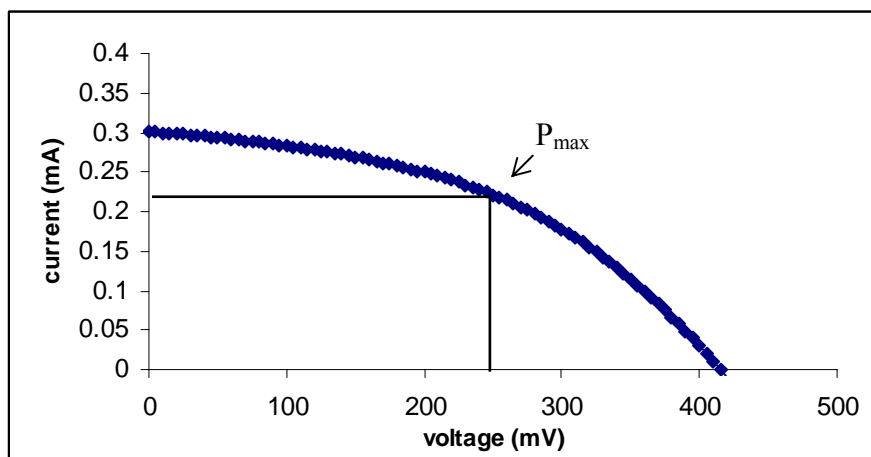


Figure 66 Current-voltage (I-V) curve of dye-sensitized solar cell that sensitized with *Monascus red*, using solid polymer electrolyte.

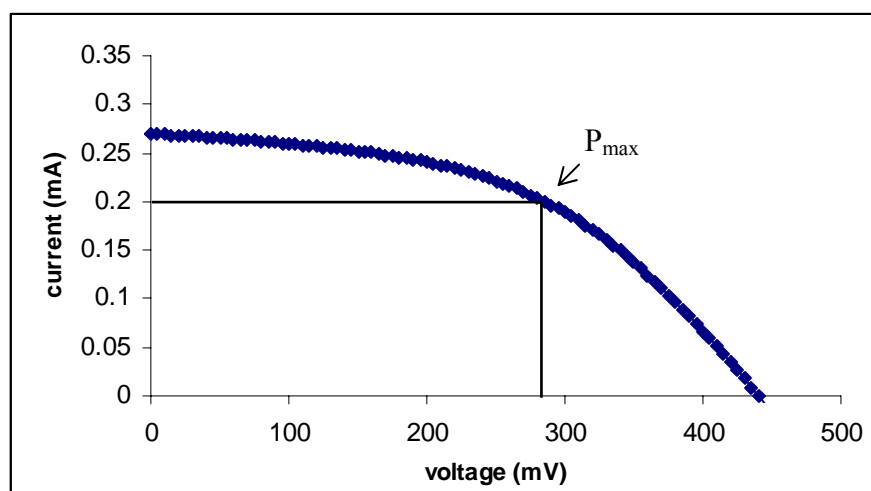


Figure 67 Current-voltage (I-V) curve of dye-sensitized solar cell that sensitized with *Monascus yellow*, using solid polymer electrolyte.

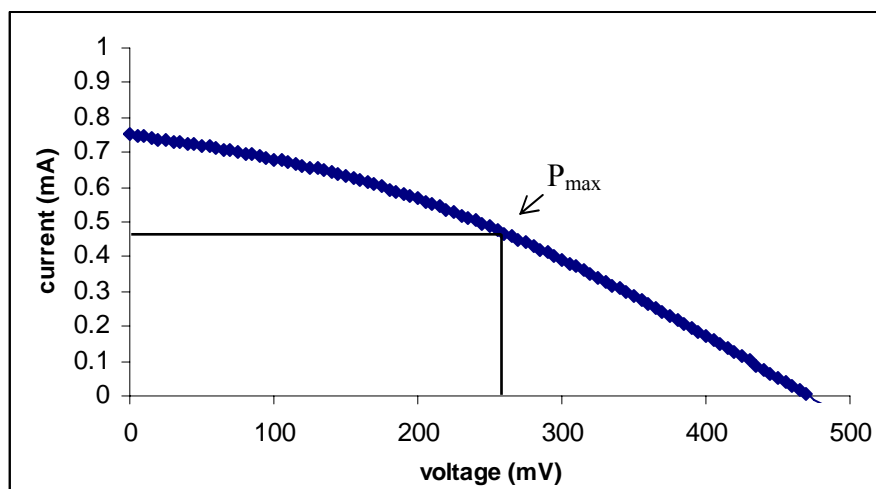


Figure 68 Current-voltage (I-V) curve of dye-sensitized solar cell that sensitized with mixture of roselle and turmeric dyes, using solid polymer electrolyte.

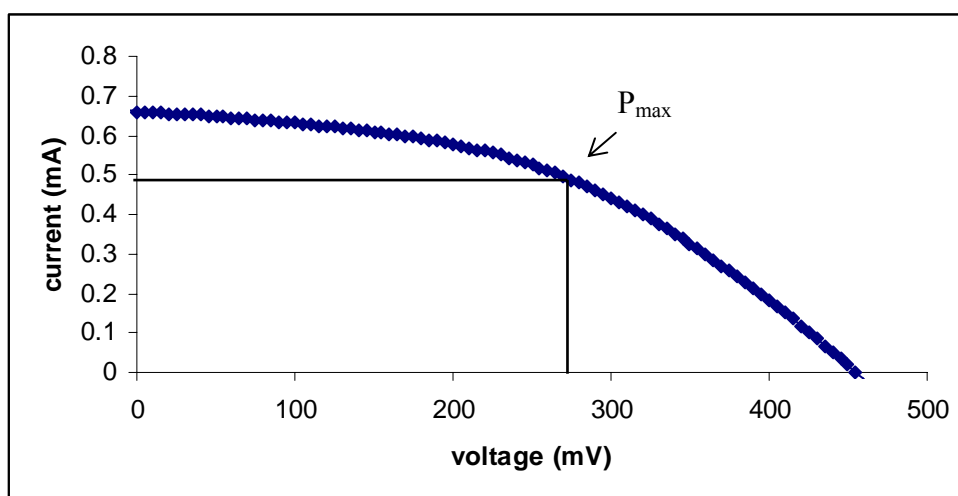


Figure 69 Current-voltage (I-V) curve of dye-sensitized solar cell that sensitized with mixture of roselle and *Monascus* red dyes, using solid polymer electrolyte.

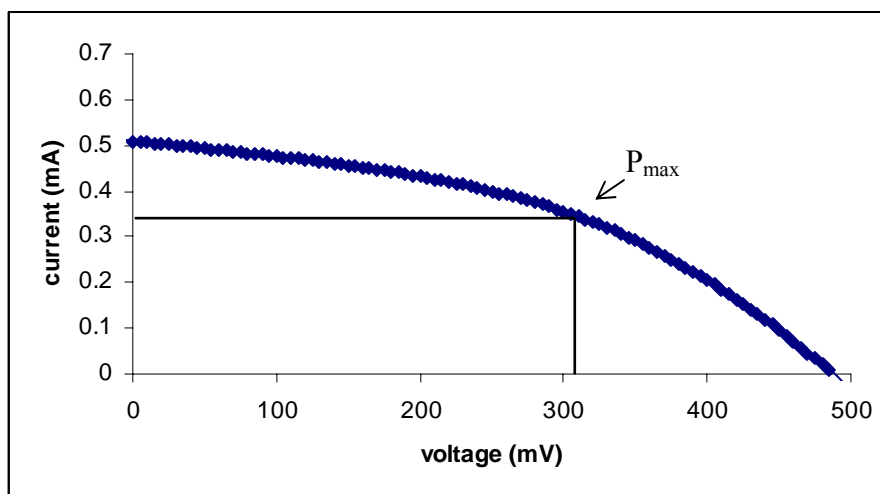


Figure 70 Current-voltage (I-V) curve of dye-sensitized solar cell that sensitized with mixture of roselle and *Monascus* yellow dyes, using solid polymer electrolyte.

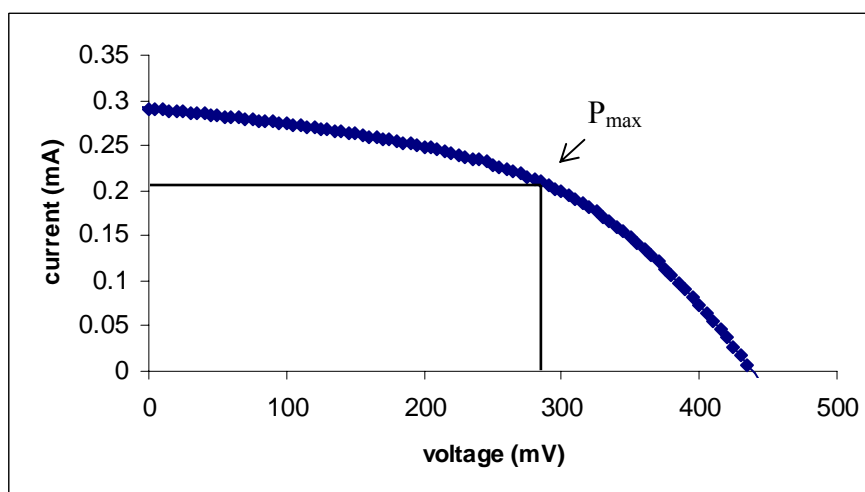


Figure 71 Current-voltage (I-V) curve of dye-sensitized solar cell that sensitized with mixture of turmeric and *Monascus* red dyes, using solid polymer electrolyte.

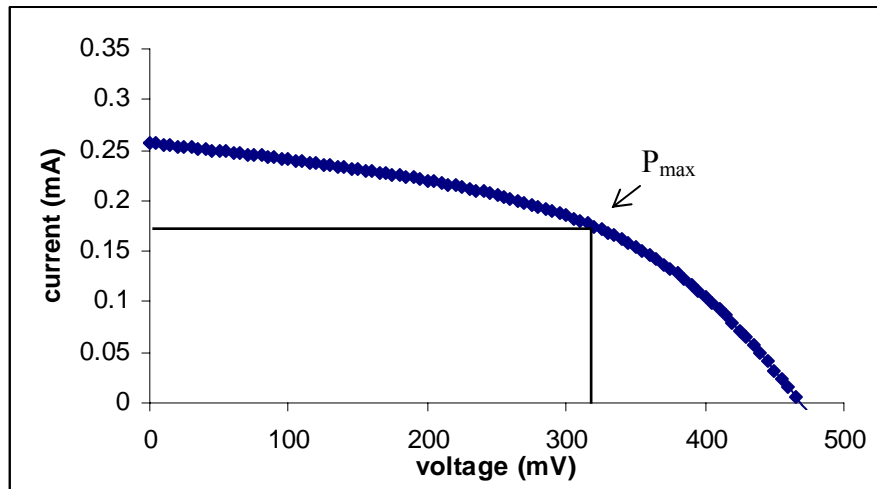


Figure 72 Current-voltage (I-V) curve of dye-sensitized solar cell that sensitized with mixture of turmeric and *Monascus* yellow dyes, using solid polymer electrolyte

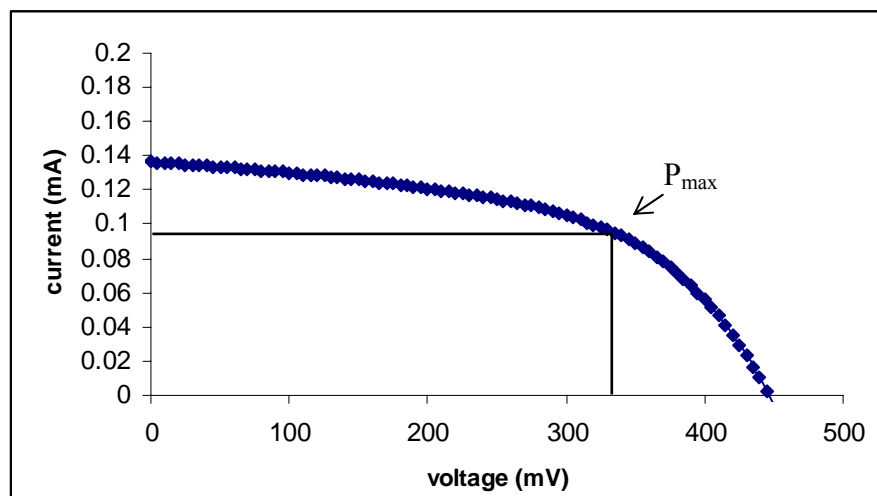


Figure 73 Current-voltage (I-V) curve of dye-sensitized solar cell that sensitized with mixture of *Monascus* red and *Monascus* yellow dyes, using solid polymer electrolyte

4.7 The Current-voltage (I-V) curves of dye-sensitized solar cell sensitized with Ru complex (N3) dye (sample 7, 8) that monitored under an illuminator (3,000 K) with active area of cell of 1cm² are shown in Figure 74- Figure 75

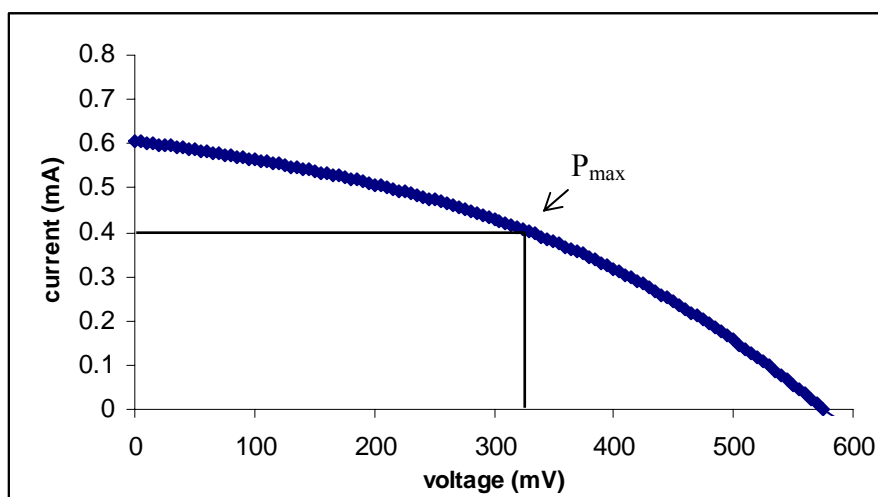


Figure 74 Current-voltage (I-V) curve of dye-sensitized solar cell that sensitized with Ru complex (N3) dye (sample 7), using solid polymer electrolyte.

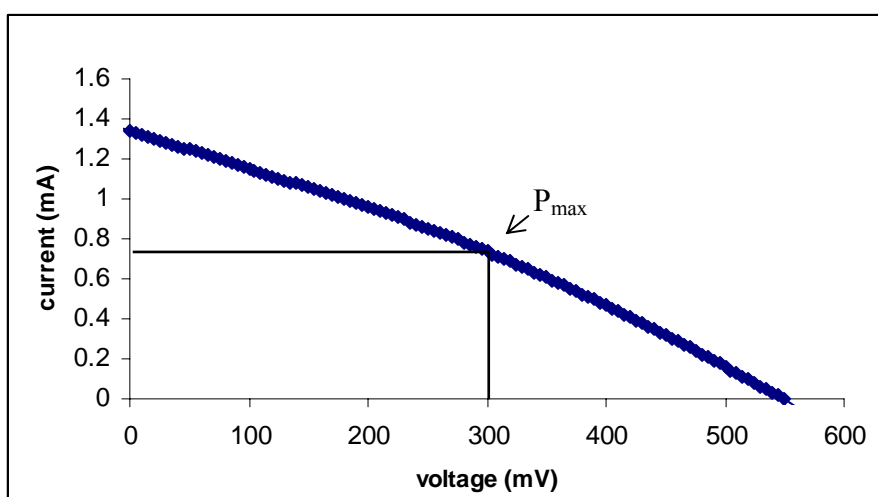


Figure 75 Current-voltage (I-V) curve of dye-sensitized solar cell that sensitized with Ru complex (N3) dye (sample 8), using solid polymer electrolyte.

5. Effect of light intensity of the sun on out put power (I_{sc} and V_{oc}) of the assembled dye-sensitized solar cells

5.1 The short-circuit current (I_{sc}) and open-circuit voltage (V_{oc}) of dye-sensitized solar cells assembled with dyes of various concentrations (batch 2) were measured at different hour of the day on exposure under the sun and are shown in Figure 76 to Figure 80.

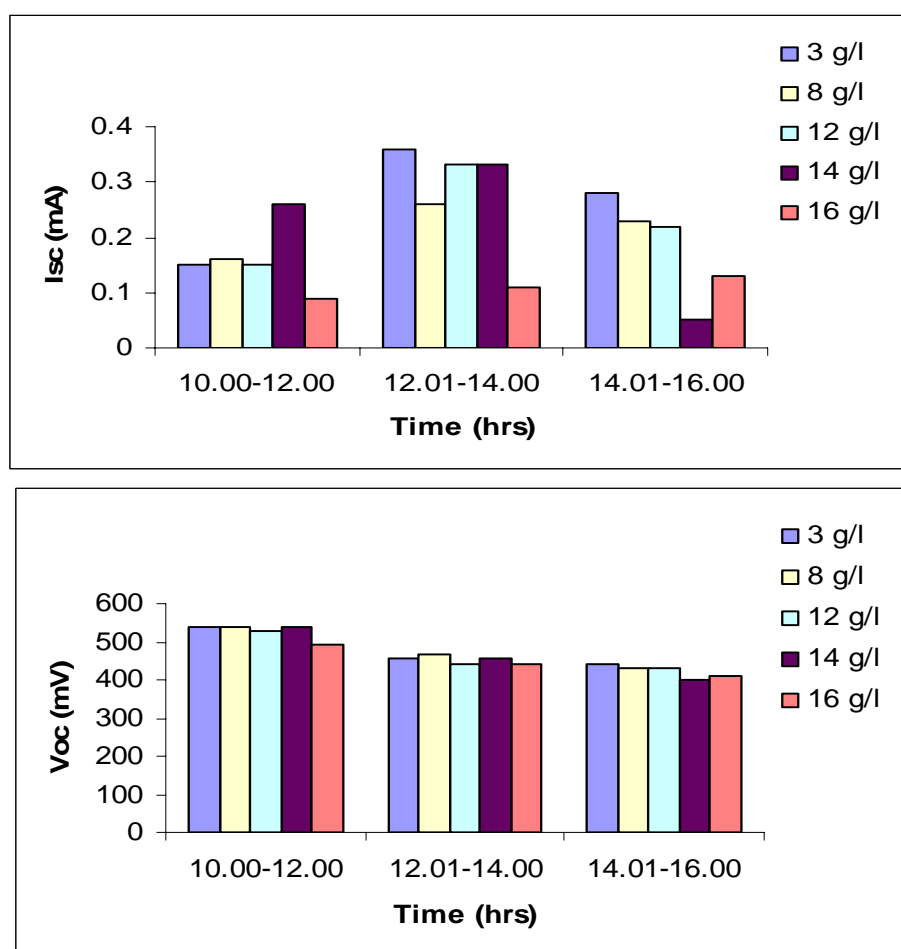


Figure 76 Variation of short-circuit current (I_{sc}) and open-circuit voltage (V_{oc}) of TiO_2 solar cells sensitized with various concentrations of roselle on measuring under the sun at different hour of the day.

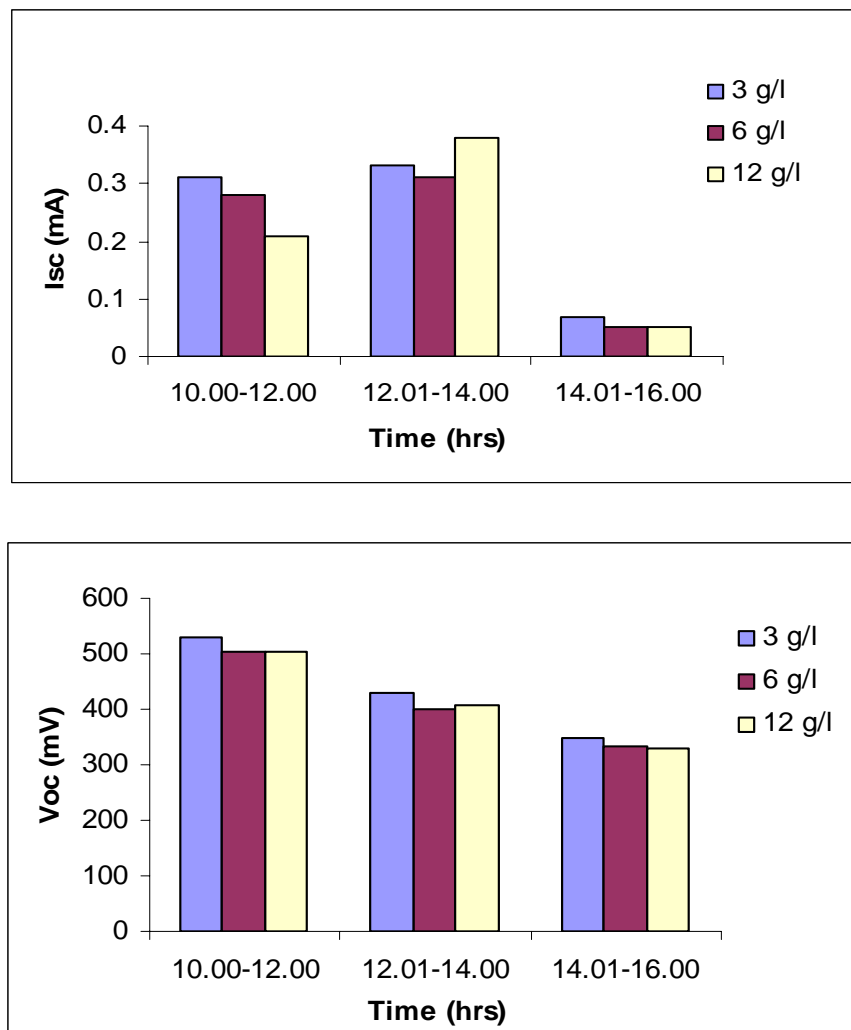


Figure 77 Variation of short-circuit current (I_{sc}) and open-circuit voltage (V_{oc}) of TiO_2 solar cells sensitized with various concentrations of turmeric on measuring under the sun at different hour of the day.

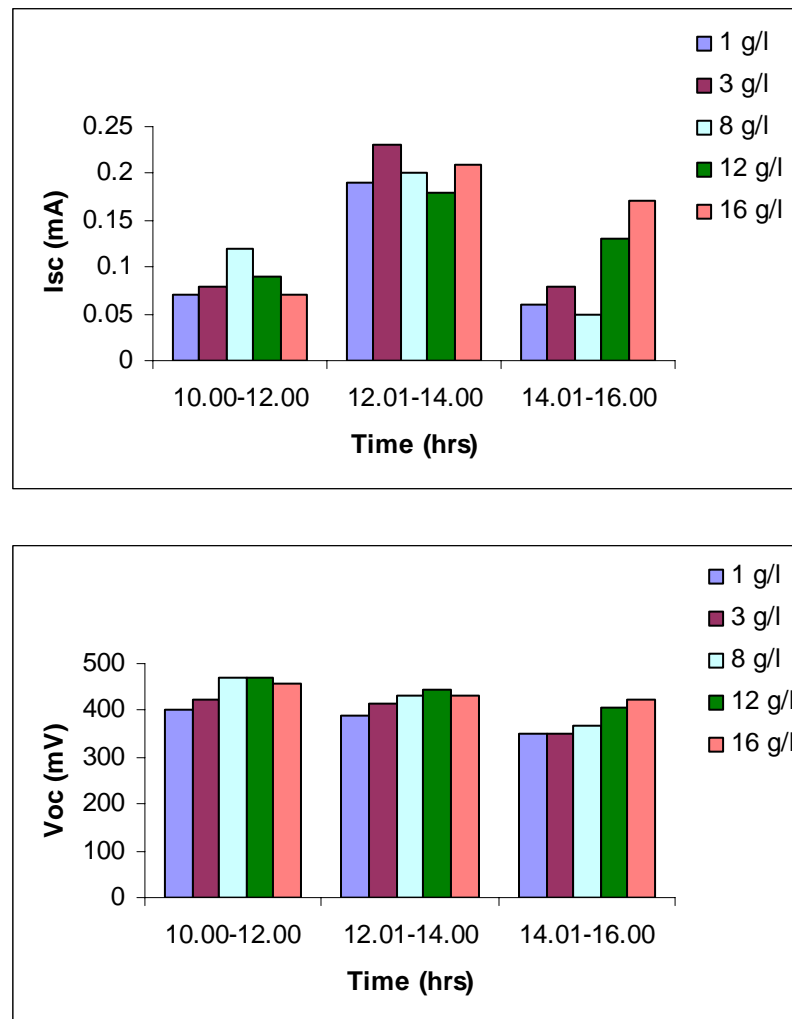


Figure 78 Variation of short-circuit current (I_{sc}) and open-circuit voltage (V_{oc}) of TiO_2 solar cells sensitized with various concentrations of *Monascus* red on measuring under the sun at different hour of the day.

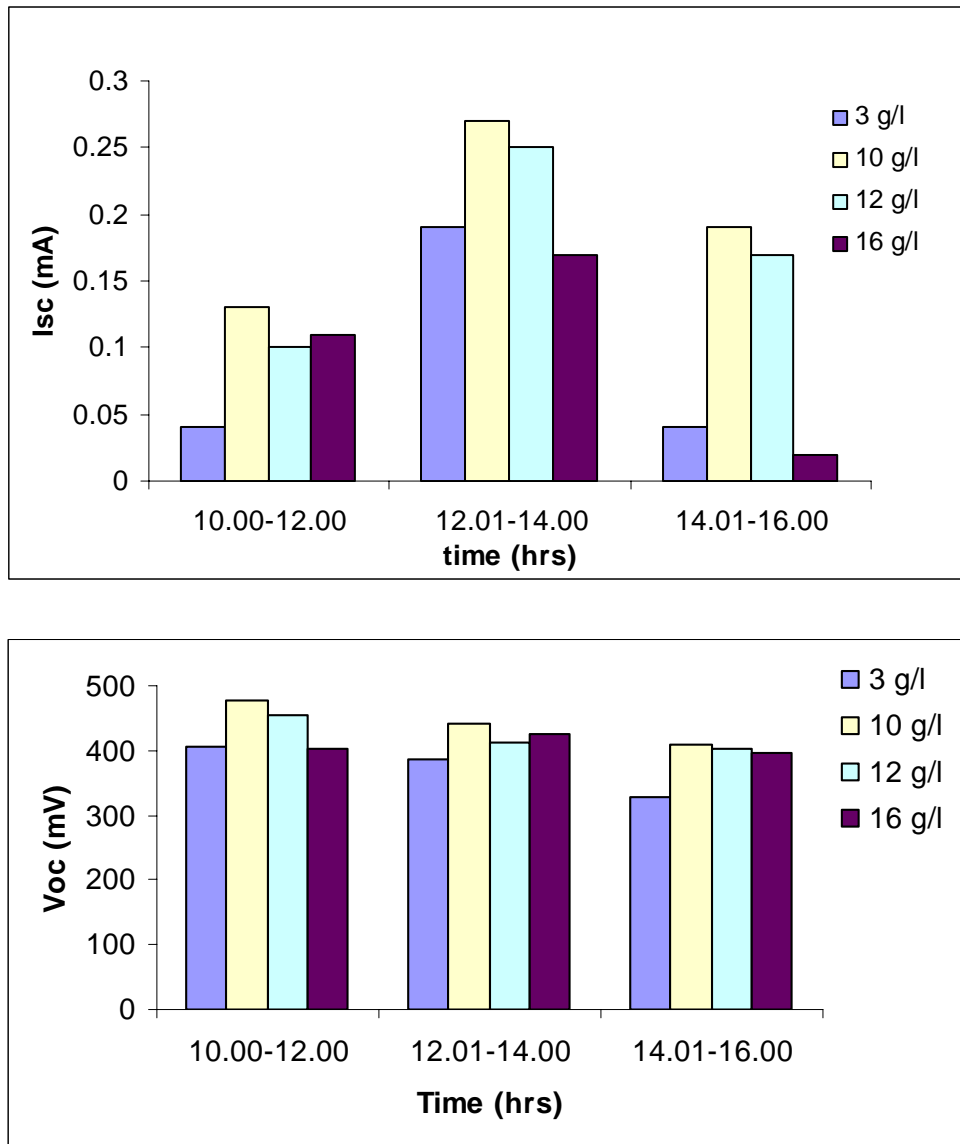


Figure 79 Variation of short-circuit current (I_{sc}) and open-circuit voltage (V_{oc}) of TiO_2 solar cells sensitized with various concentrations of *Monascus* yellow on measuring under the sun at different hour of the day.

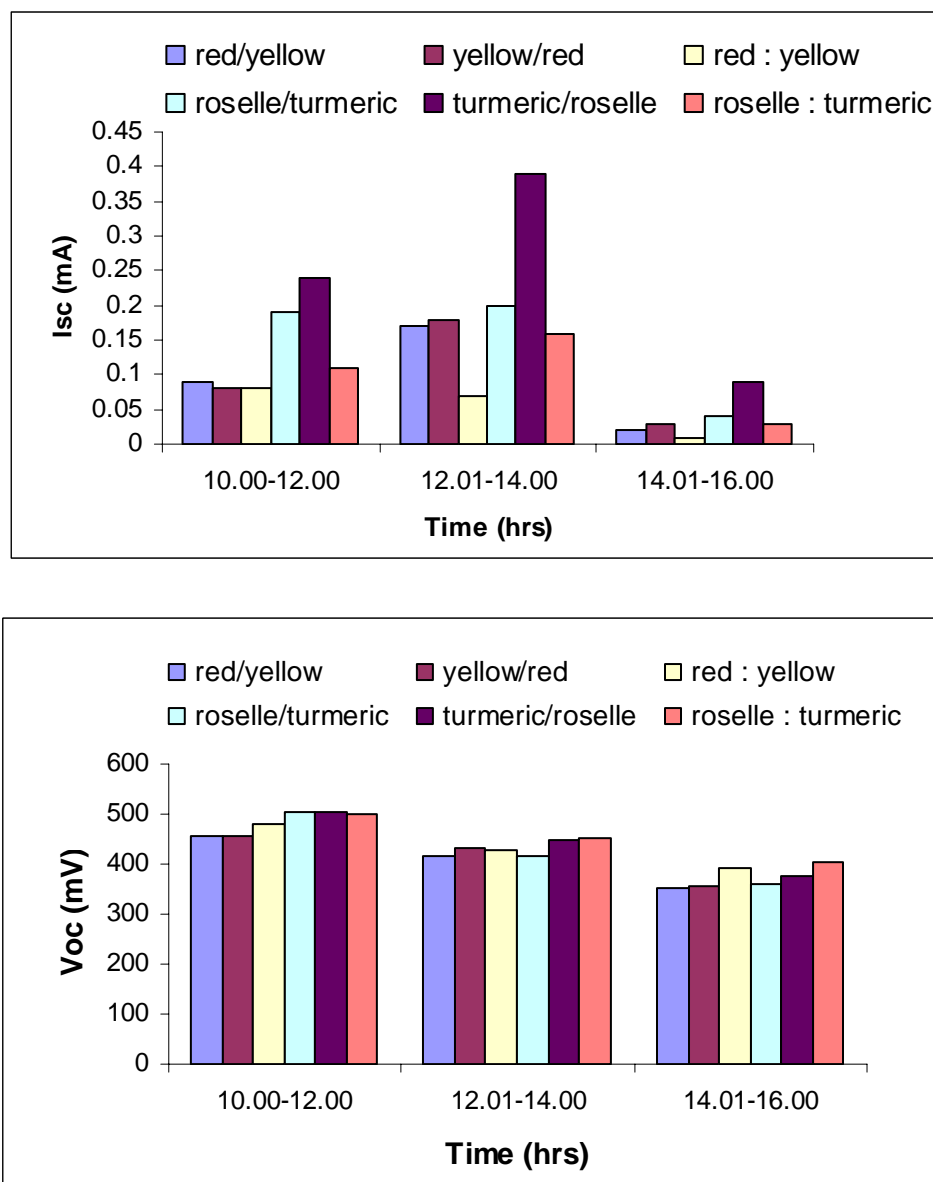


Figure 80 Variation of short-circuit current (I_{sc}) and open-circuit voltage (V_{oc}) of TiO_2 solar cells sensitized with mixture of dyes on measuring under the sun at different hour of the day.

The results from Figure 76 to Figure 80 show that the values of short-circuit current (I_{sc}) were increased when the light intensity of the sun was increased since highest values of short-circuit current (I_{sc}) were observed during noon time on a full bright day. The values of open-circuit voltage (V_{oc}) were slightly decreased on longer time of exposure under the sun due to an increase in cell temperature.

5.2 The short-circuit current (I_{sc}) of dye-sensitized solar cells assembled with roselle, turmeric, *Monascus* red, *Monascus* yellow and mixture of dyes (batch 5) were measured at different hour of the day on exposure under the sun for 3 days and are shown in Figure 81 to Figure 83.

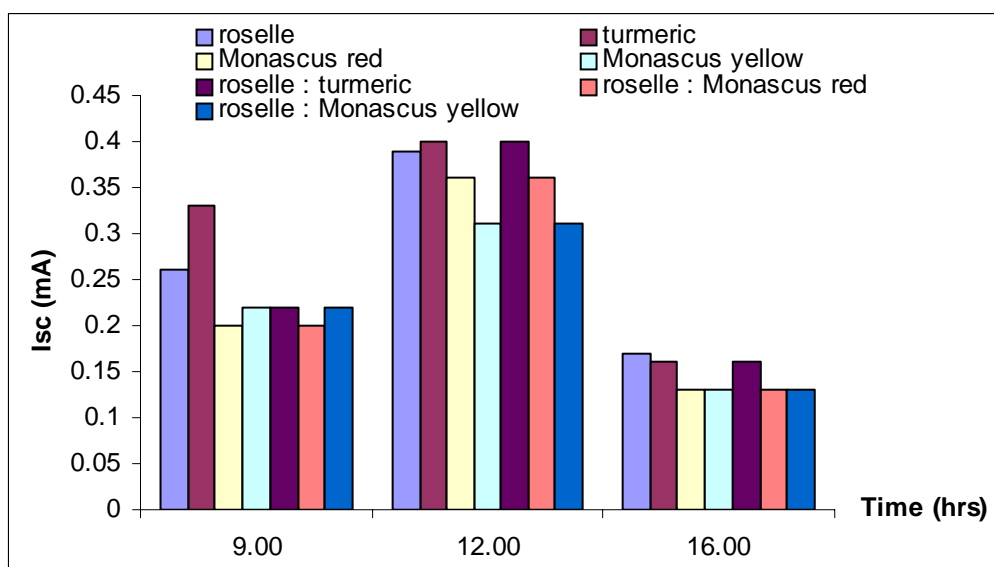


Figure 81 Variation of short-circuit current (I_{sc}) of TiO_2 solar cells sensitized with roselle, turmeric, *Monascus* red, *Monascus* yellow and mixture of dyes (batch 5) on measuring under the sun at different hour of the day. (day 1, a full bright day)

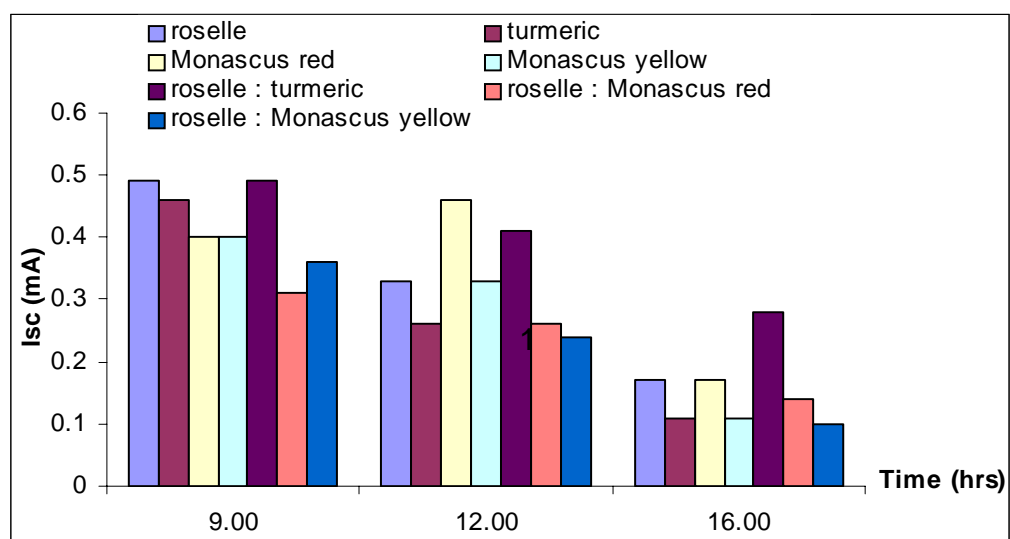


Figure 82 Variation of short-circuit current (I_{sc}) of TiO_2 solar cells sensitized with roselle, turmeric, *Monascus* red, *Monascus* yellow and mixture of dyes (batch 5) on measuring under the sun at different hour of the day. (day 2 cloudy in the afternoon)

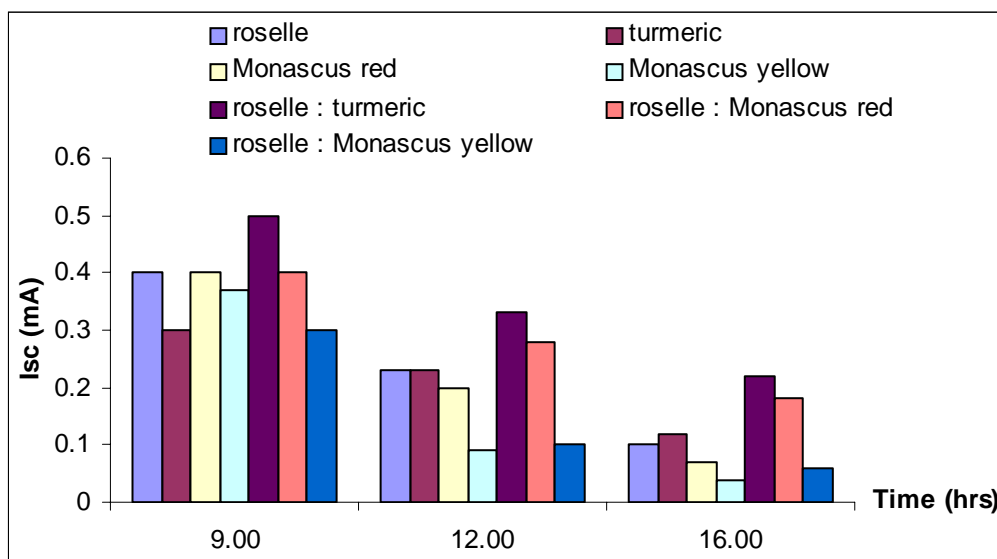


Figure 83 Variation of short-circuit current (I_{sc}) of TiO_2 solar cells sensitized with roselle, turmeric, *Monascus* red, *Monascus* yellow and mixture of dyes (batch 5) on measuring under the sun at different hour of the day. (day 3, cloudy in the afternoon)

The results from Figure 81- Figure 83 show that the values of short-circuit current (I_{sc}) were increased when the light intensity of the sun was increased since highest values of short-circuit current (I_{sc}) were observed during 12.00 hr. on a full bright day.

5.3 The short-circuit current (I_{sc}) of dye-sensitized solar cells assembled with Ru complex (N3) dye (sample 5) were measured at different hour of the day on exposure under the sun for 3 days and are shown in Figure 84.

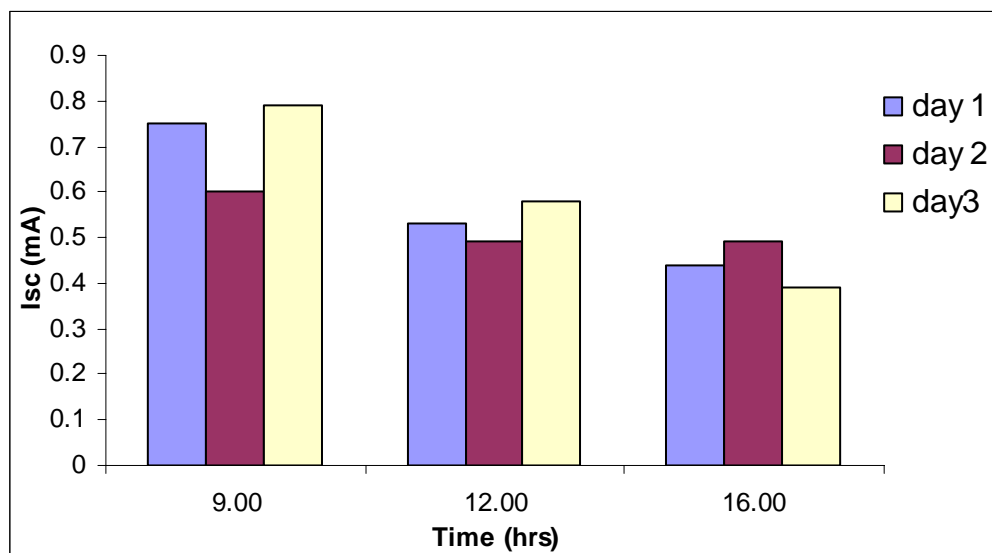


Figure 84 Variation of short-circuit current (I_{sc}) of TiO_2 solar cells sensitized with Ru complex (N3) dye (sample 8 batch5) on measuring under the sun at different hour of the day for 3 days (cloudy in the afternoon)

The results from Figure 84 show that the values of short-circuit current (I_{sc}) were increased when the light intensity of the sun was increased since highest values of short-circuit current (I_{sc}) were observed during 9.00 hr. on cloudy in the afternoon day.

6. Durability of the assembled dye-sensitized solar cell

6.1 The durability of dye-sensitized solar cells assembled with roselle, turmeric, *Monascus* red and *Monascus* yellow dyes at various concentrations of dye solution are investigated by measurements of the short-circuit current (I_{sc}) with an illuminator after exposing under the sun and are shown in Figure 85 to Figure 88.

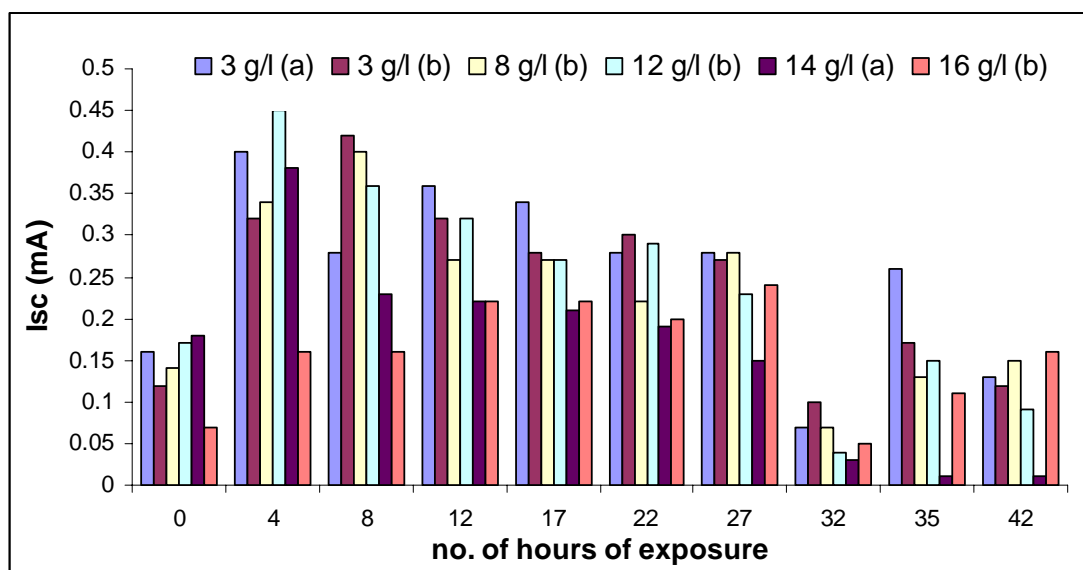


Figure 85 Short-circuit current (I_{sc}) measured with an illuminator (3,000 K) after exposing the TiO_2 solar cell sensitized with various concentrations of roselle under the sun at various hours

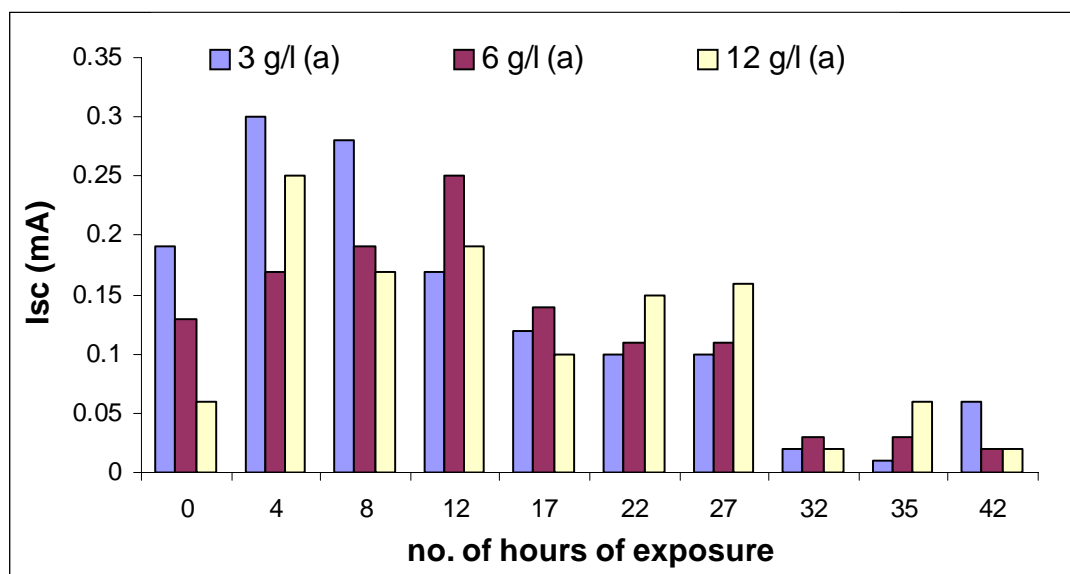


Figure 86 Short-circuit current (I_{sc}) measured with an illuminator (3,000 K) after exposing the TiO_2 solar cell sensitized with various concentrations of turmeric under the sun at various hours

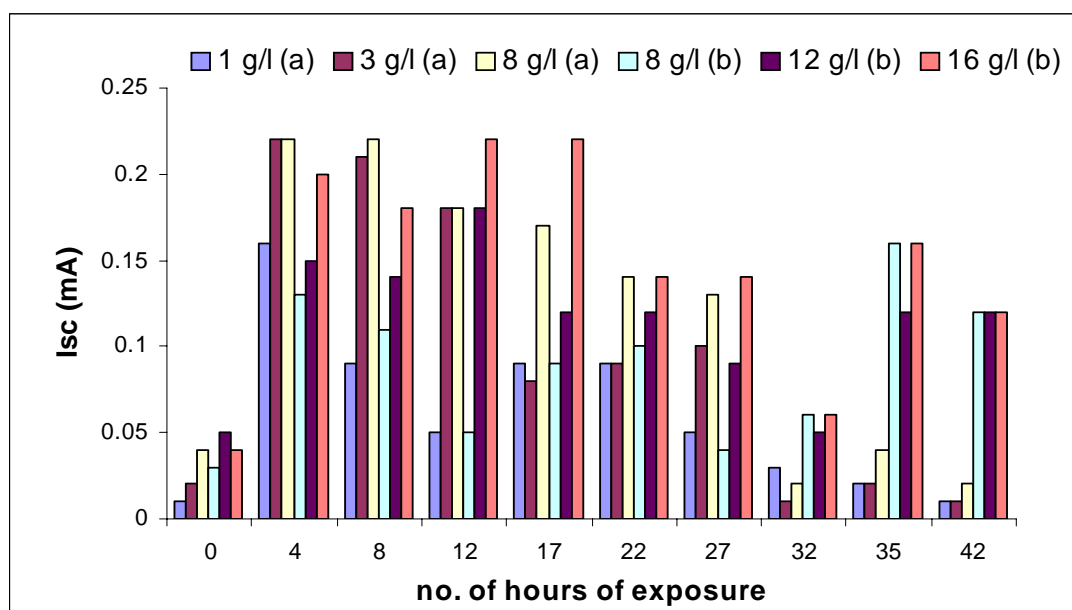


Figure 87 Short-circuit current (I_{sc}) measured with an illuminator (3,000 K) after exposing the TiO_2 solar cell sensitized with various concentrations of *Monascus* red under the sun at various hours

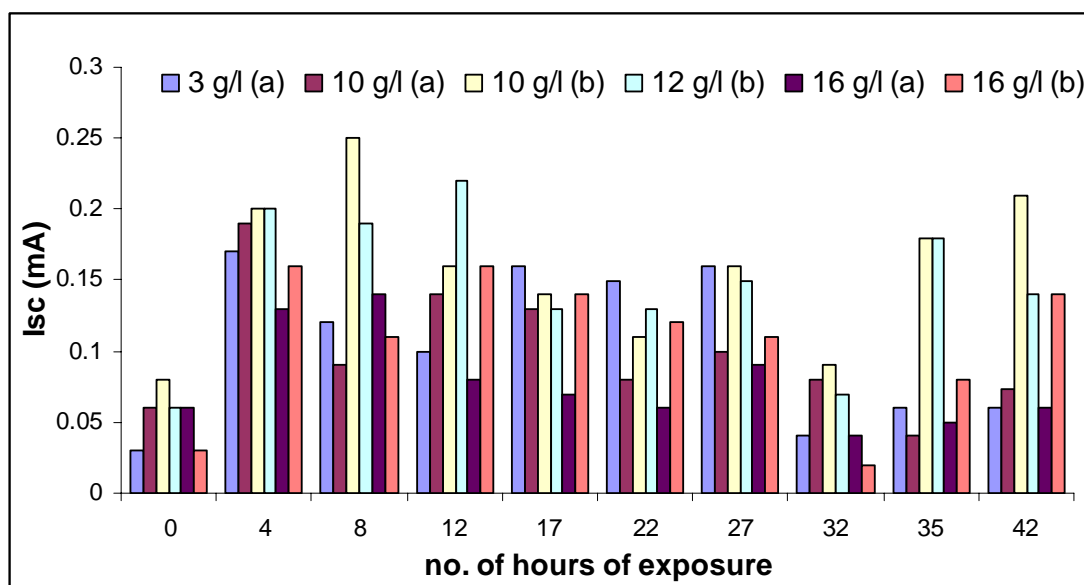


Figure 88 Short-circuit current (I_{sc}) measured with an illuminator (3,000 K) after exposing the TiO_2 solar cell sensitized with various concentrations of *Monascus* yellow under the sun at various hours

The results from Figure 85 to Figure 88 showed that the short-circuit current (I_{sc}) was increased on the first 8-12 hours of exposure because the solid polymer electrolyte was softened under exposure to the sun and thus gave rise to better contact of the photoelectrode and the electrolyte.

6.2 The durability of dye-sensitized solar cells assembled with roselle, turmeric, *Monascus* red and *Monascus* yellow dyes (batch 5) are investigated by measurements of the short-circuit current (I_{sc}) with an illuminator after exposing under the sun and are shown in Figure 89

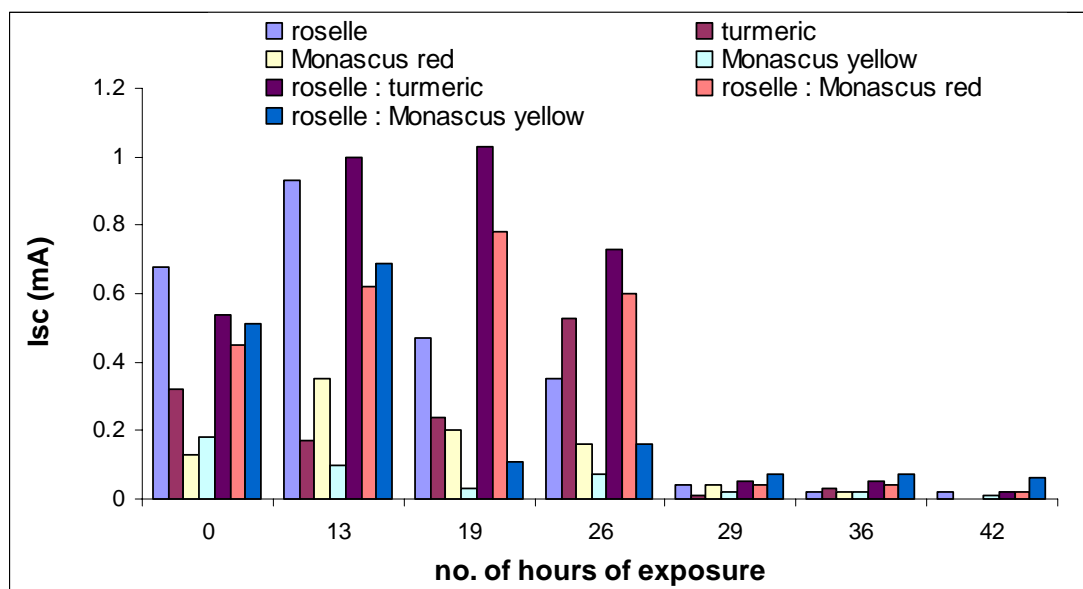


Figure 89 Short-circuit current (I_{sc}) measured with an illuminator (3,000 K) after exposing the TiO_2 solar cell sensitized with dyes (batch 5) under the sun at various hours

The results from Figure 89 showed that the short-circuit current (I_{sc}) was increased on the first 13-19 hours of exposure because the solid polymer electrolyte was softened under exposure to the sun and thus gave rise to better contact of the photoelectrode and the electrolyte. The dye-sensitized solar cells were eventually degraded after 29 hours (approximately 4 days) of exposure. This due to the leakage and the evaporation of electrolyte and the degradation of natural dye extracts in dye-sensitized solar cells.

6.3 The durability of dye-sensitized solar cells assembled with Ru complex (N3) dye are investigated by measurements of the short-circuit current (I_{sc}) with an illuminator after exposing under the sun and are shown in Figure 90.

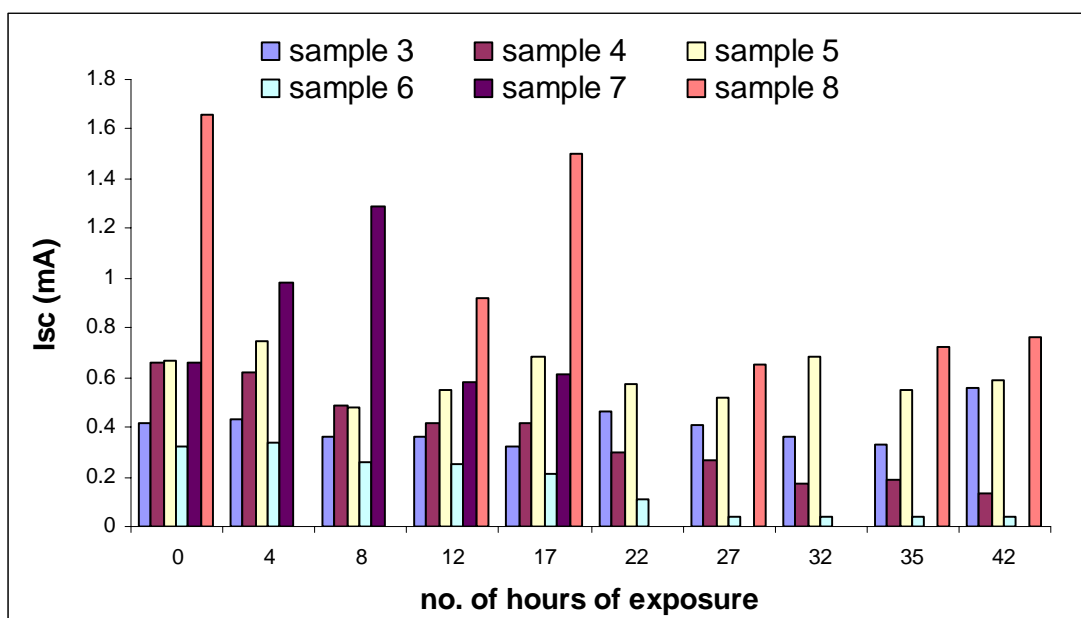


Figure 90 Short-circuit current (I_{sc}) measured with an illuminator (3,000 K) after exposing the TiO_2 solar cell sensitized with N3 dye under the sun at various hours

The results from Figure 90 showed that the short-circuit current (I_{sc}) was decreased on the 22 hours of exposure because of the leakage and the evaporation of electrolyte in dye-sensitized solar cells. The dye-sensitized solar cells sensitized with N3 dye remained stable after 42 hours (approximately 7 days) of exposure to the sun.

CONCLUSION

In this work, four natural dye extracts of roselle, turmeric, *Monascus* red and *Monascus* yellow, were selected as sensitizers to be compared with a ruthenium complex $\text{RuL}_2(\text{NCS})_2$ 535 (N3) which is one of the most effective sensitizer for dye-sensitized solar cells (DSSCs) because natural dyes are readily available and much cheaper than the ruthenium complexes. The solid-state DSSC fabricated consisted of 1 cm^2 effective area of nanocrystalline titanium dioxide (degussa P25) coated on indium tin oxide (ITO) glass immersed in ethanol solution of dye extract as an anode and a platinized ITO glass as a counter electrode. The two electrodes were sandwiched with a composite of poly(ethylene) oxide filled with titanium oxide and a redox couple of KI and I_2 as solid electrolyte.

The absorption and fluorescence spectra of the dye extracts in ethanol solution were obtained in the range 300-700 nm and 550-800 nm respectively, which meet the requirement as sensitizers. Electrochemical property of dye extracts were also studied, cyclic voltammogram of roselle extract in KNO_3 solution showed quasi-reversible reduction wave at the potential of -0.62 V and oxidation wave at the potential of -0.31 V while those of other three dye extracts were not observed. This is consistent with the effectiveness of sensitization property in DSSC that among the four dye extracts, roselle extract gave highest short-circuit photocurrent (I_{sc}) of 0.94 mA cm^{-2} and an open-circuit voltage (V_{oc}) of 470 mV while others were $0.27\text{-}0.30 \text{ mA cm}^{-2}$ and 440-455 mV.

DSSCs sensitized with mixed dyes of different combination of two dyes of four types : roselle, turmeric, *Monascus* red and yellow were also fabricated and tested for their performance. The results showed that roselle dye was better sensitizer than all 6 combinations of two mixed dyes of four types and the combinations with roselle as one of the dyes were better than those without roselle dye.

The performances of DSSCs under the sun were studied by recording I_{sc} and V_{oc} at different hour of the day. The highest value of I_{sc} was obtained during noon time of a bright day when the highest intensity from the sun was obtained and the value was approximately close to the value measured with an illuminator (3000K). The V_{oc} values of each DSSC showed a slight variation and the values tended to decrease after 5-6 hours of exposure under the sun due to an increase in cell temperature.

The durability of the performance of the solid-state DSSCs was also studied by exposing the cells under the sun for several days. The I_{sc} was measured with an illuminator (3000K) after each day of exposure. The DSSCs fabricated with natural dyes as sensitizers could last for only 4 days (approximately 29 hours) while those with N3 dye as a sensitizer was still stable.

LITERATURE CITED

- Anandan, S., S. Latha, S. Murugesan, J. Madhavan, B. Muthuraaman and P. Maruthamuthu. 2005. Synthesis, characterization and fabrication of solar cells making use of [Ru(dcbpy)(tptz)X]X (where X= Cl⁻, SCN⁻, CN⁻) complexes. **Solar Energy**. 79: 440-448.
- Amao, Y., Y. Yamada and K. Aoki. 2004. Preparation and properties of dye-sensitized solar cell using chlorophyll derivative immobilized TiO₂ film electrode. **J. Photochem. Photobiol. A: Chem.** 164: 47-51.
- Amao, Y. and T. Komori. 2004. Bio-photovoltaic conversion device using chlorine-e₆ derived from chlorophyll from *Spirulina* adsorbed on a nanocrystalline TiO₂ film electrode. **Biosensors and Bioelectronics**. 19: 843-847.
- Chatzivasiloglou, E., T. Stergiopoulos, N. Spyrellis and P. Falaras. 2005. Solid-state sensitized solar cells, using [Ru(dcbpyH₂)₂Cl₂·2H₂O as the dye and PEO/titania/I⁻/I₃⁻ as the redox electrolyte. **Journal of Materials Processing Technology**. 161: 234-240.
- Chen, X., J. Guo, X. Peng, M. Guo, Y. Xu, L. Shi, C. Liang, L. Wang, Y. Gao, S. Sun and S. Cai. 2005. Novel cyanine dyes with different methane chains as sensitizers for nanocrystalline solar cell, **J. Photochem. Photobiol. A: Chem.** 171:235-240.
- Cherepy, N.J., G.P. Smestad, M. Grätzel and J.Z. Zhang. 1997. Ultrafast Electron Injection: Implications for a photoelectrochemical Cell Utilizing an Anthocyanin Dye-Sensitized TiO₂ Nanocrystalline Electrode. **J. Phys. Chem. B.** 101: 9342-9351.
- Du, C.T. and F. J. Francis. 1973. Anthocyanins of Roselle (*Hibiscus sabdariffa*, L.). **Journal of food science**. 38: 810-812.
- Dai, Q. and J. Rabani. 2002. Photosensitization of nanocrystalline TiO₂ films by anthocyanin dyes. **J. Photochem. Photobiol. A: Chem.** 148: 17-24.
- Esteves, F., and E. P. Cunha. Voltammetric study and electrochemical degradation of reactive dyes. **5th World Textile Conference AUTEX 2005**. Portoroz, Slovenia 2005.

- Garcia, C.G., A. Sarto and N.Y.M. Iha. 2003. Fruit extracts and ruthenium polypyridinic dyes for sensitization of TiO₂ in photoelectrochemical solar cells. **J. Photochem. Photobiol. A: Chem.** 160: 87-91.
- Gassama-Dia, Y. K., D. Sané and M. Ndoye. 2004. Direct genetic transformation of *Hibiscus sabdariffa*, L. **African Journal of Biotechnology.** 3(4): 226-228.
- Grätzel, M. 2004. Conversion of sunlight to electric power by nanocrystalline dye-sensitized solar cells. **J. Photochem. Photobiol. A: Chem.** 164: 3-14.
- Greijer, A. H., 2003. Interactions in dye-sensitized solar cells. **Comprehensive summaries of Uppsala dissertations.** Uppsala University
- Guaratini, C. C. I., A. G. Fogg and M. V. B. Zanoni. 2001. Studies of the voltammetric behavior and determination of diazo reactive dyes at mercury electrode. **Electroanalysis.** 13(18): 1535-1543.
- Halme, J. 2002. Dye-sensitized nanostructured and organic photovoltaic cells: technical review and preliminary tests. **Master's thesis.** Helsinki University of Technology.
- Hao, S., J. Wu, Y. Huang and J. Lin. 2006. Natural dyes as photosensitizers for dye-sensitized solar cell. **Solar Energy.** 80: 209-214.
- Hinsch, A., et al. 2000. Long-term stability of dye sensitized solar cells for large area power applications (BATCHE-DSC). **16th European Photovoltaic Solar Energy Conference and Exhibition.** Glasgow 2000
- Jana, A. K. 2000. Solar cells based on dyes. **J. Photochem. Photobiol. A: Chem.** 132 : 1-17.
- Jana, A.K. and B.B. Bhowmik. 1999. Enhancement in power output of solar cells consisting of mixed dyes. **J. Photochem. Photobiol. A: Chem.** 122: 53-56.
- Jayaweera, P.M., S.S. Palayangoda and K. Tennakone. 2001. Nanoporous TiO₂ solar cells sensitized with iron (II) complexes of bromopyrogallol red ligand. **J. Photochem. Photobiol. A: Chem.** 140: 173-177.

- Jongrungruangchok, S., P. Kittakoop, B. Yongsmith, R. Bavovada, S. Tanasupawat, N. Lartpornmatulee and Y. Thebtaranonth. 2004. Azaphilone pigments from a yellow mutant of fungus *Monascus kaoliang*. **Phytochemistry** 65: 2569-2575.
- Kalyanasundaram, K. and M. Grätzel. 1998. Applications of functionalized transition metal complexes in photonic and optoelectronic. **Coord. Chem. Rev.** 77: 347-414.
- Kim, D., Y. Jeong, S. Kim, D. Lee and J. Song. 2005. Photovoltaic performance of dye-sensitized solar cell assembled with gel polymer electrolyte. **J. Power Sources.** 149: 112-116.
- Kumara, G. R. A., S. Kaneko, M. Okuya, B. Onwona-Agyeman, A. Konno and K. Tennakone. 2006. Shiso leaf pigments for dye-sensitized solid-state solar cell. **Sol. Energy Mat. Sol cells.** 90: 1220-1226.
- Li, W., J. Kang, X. Li, Y. Lin, G. Wang and X. Xiao. 2005. A novel polymer quaternary ammonium iodide and application in quasi-solid-state dye-sensitized solar cells. **J. Photochem. Photobiol. A: Chem.** 170: 1-6.
- Matsui, M., Y. Hashimoto, K. Funabiki, J. Jin, T. Yoshida and H. Minoura. 2005. Application of near-infrared absorbing heptamethine cyanine dyes as sensitizers for zinc oxide solar cell. **Synthetic Metals.** 148: 147-153.
- Matsubara, T., Y. Ichikawa, K. Aramaki and A. Katagiri. 2005. The use of xylene orange in dye-sensitized solar cell. **Sol. Energy Mat. Sol cells.** 85: 269-275.
- Mosurkal, R., J. He, K. Yang, L. A. Samuelson and J. Kumar. 2004. Organic photosensitizers with catechol groups for dye-sensitized solar photovoltaics. **J. Photochem. Photobiol. A: Chem.** 168: 191-196.
- Nazeeruddin, M. K., A. Kay, I. Rodicio, R. Humphry-Baker, E. Müller, P. Liska, N. Vlachopoulos and M. Grätzel. 1993. Conversion of light to electricity by *cis*-X₂Bis(2,2'-bipyridyl-4,4'-dicarboxylate)ruthenium(II) charge-transfer sensitizers (X = Cl⁻, Br⁻, I⁻, CN⁻, and SCN⁻) on nonacrySTALLINE TiO₂ electrodes. **J. Am. Chem. Soc.** 115: 6382-6390.

- Nazeeruddin, M. K., C. Klein, P. Liska and M. Grätzel. 2005. Synthesis of novel ruthenium sensitizers and their application in dye-sensitized solar cells. **Coord. Chem. Rev.** 249: 1460-1467.
- Olea, A., G. Ponce and P.J. Sebastian. 1999. Electron transfer via organic dyes for solar conversion. **Solar Sol. Energy Mat. Sol cells.** 59: 137-143.
- Otaka, H., M. Kira, K. Yano, S. Ito, H. Mitekura, T. Kawata, and F. Matsui. 2004. Multi-colored dye sensitized solar cells. **J. Photochem. Photobiol. A: Chem.** 164: 67-73.
- Perera, V. P. S., P. K. D. D. P. Pitigala, M. K. I. Senevirathne and K. Tennakone. 2005. A solar cell sensitized with three different dyes. **Solar Sol. Energy Mat. Sol cells.** 85: 91-98.
- Polo. A. S., M. K. Itokazu and N. Y. M. Iha. 2004. Metal complex sensitizers in dye-sensitized solar cells. **Coord. Chem. Rev.** 248: 1343-1361.
- Roberts, S. 1991. **Solar electricity.** 1st ed., Prentice Hall International (UK) Ltd., 19-28 pp.
- Smestad, G.P., and M. Grätzel. 1998. Demonstrating electron transfer and nanotechnology: A natural dye-sensitized nanocrystalline energy converter. **J. Chem. Educ.** 75(6): 752-756.
- Smestad, G.P. 1998. Education and solar conversion: Demonstrating electron transfer. **Solar Sol. Energy Mat. Sol cells.** 55: 157-178.
- Yao, Q.H., F.S. Meng, F.Y. Li, H. Tian and C.H. Huang. 2003. Photoelectric conversion properties of four novel carboxylated hemicyanine dyes on TiO₂ electrode. **J. Mater. Chem.** 13: 1048-1053.
- Yongsmith, B., V. Kitprechavanich, L. Chitradon, C. Chairisook and N. Budda. 2000. Color mutants of *Monascus* sp. KB9 and their comparative glucoamylases on rice solid culture. **J. Mol. Catal. B: Enzymatic.** 10: 263-272.
- Zanoni, M. V. B., A. G. Fogg, J. Barek and J. Zima. 1995. Electrochemical investigations of reative dyes; polarographic determination of anthraquinone-based chlorotriazine dyes. **Anal. Chim. Acta.** 315: 41-54.

